# Plate-boundary earthquakes and tsunamis of the past 5500 yr, Sixes River estuary, southern Oregon

**Harvey M. Kelsey***
*Department of Geology, Humboldt State University, Arcata, California 95521, USA*

**Robert C. Witter**
*William Lettis and Associates, Inc., 1777 Botelho Drive, Suite 262, Walnut Creek, California 94596, USA*

**Eileen Hemphill-Haley**
*Department of Geology, Humboldt State University, Arcata, California 95521, USA*

## ABSTRACT

**Eleven plate-boundary earthquakes over the past 5500 yr have left a stratigraphic signature in coastal wetland sediments at the lower Sixes River valley in south coastal Oregon. Within a 1.8 km² abandoned meander valley, 10 buried wetland soils record gradual and abrupt relative sea-level changes back in time to ~6000 yr ago. An additional, youngest buried soil at the mouth of the Sixes River subsided during the A.D. 1700 Cascadia earthquake. Multiple lines of evidence indicate that tectonic subsidence caused soil burial, including permanent relative sea-level rise following burial, lateral continuity of buried soil horizons over hundreds of meters, diatom assemblages showing that sea level rose abruptly at least 0.5 m, and sand deposits on top of buried soils demonstrating coincidence of coseismic subsidence and tsunami inundation. For at least two of the buried soils, liquefaction of sediment accompanied subsidence.**

**The 11 soil-burial events took place between 300 and ~5400 yr ago, yielding an average recurrence interval of plate-boundary earthquakes of ~510 yr. Comparing paleoseismic sites in southern Washington and south coastal Oregon with the Sixes River site for the past 3500 yr indicates that the number and timing of recorded plate-boundary earthquakes are not the same at all sites. In particular, a Sixes earthquake at ~2000 yr ago lacks a likely correlative in southern Washington. Therefore, unlike the A.D. 1700 Cascadia earthquake, some Cascadia plate-boundary earthquakes do not rupture the entire subduction zone from southern Oregon to southern Washington.**

**In the lower Sixes River valley, the upper-plate Cape Blanco anticline deforms sediment of late Pleistocene and Holocene age directly above the subduction zone. Differential tectonic subsidence occurred during two of the plate-boundary earthquakes when a blind, upper-plate reverse fault, for which the Cape Blanco anticline is the surface fold, slipped coseismically with rupture of the plate boundary. During these two earthquakes, sites ~2 km from the anticline axis subsided ~0.5 m more than sites ~1 km from the axis.**

**Keywords: buried soils, Cascadia subduction zone, paleoseismology, plate boundaries, subduction zones, tsunamis.**

## INTRODUCTION

The Cascadia subduction zone generates plate-boundary earthquakes as large as magnitude 9 (Atwater et al., 1995; Satake et al., 1996; Clague, 1997). Even though the subduction zone has no historic record of repeated plate-boundary earthquakes, stratigraphic records of abrupt relative sea-level changes along Cascadia (Darienzo and Peterson, 1990; Atwater and Hemphill-Haley, 1997; Nelson et al., 1998) archive repeated episodes of widespread, coseismic subsidence caused by Cascadia plate-boundary earthquakes in the past 3000 yr.

Although the Cascadia margin generates plate-boundary earthquakes of magnitude 8 or greater, questions remain concerning the recurrence interval and rupture extent of Cascadia plate-boundary earthquakes and the seismic role of upper-plate structures. With only one published record of Cascadia plate-boundary earthquakes that is as long as 3500 yr (Atwater and Hemphill-Haley, 1997), more long earthquake records are needed to establish recurrence-interval estimates. Rupture extents of individual plate-boundary earthquakes are poorly understood. An earthquake in A.D. 1700 probably ruptured the entire Cascadia margin (Satake et al., 1996; Jacoby et al., 1997; Yamaguchi et al., 1997). However, limited published records of older Cascadia plate-boundary earthquakes leave open the question of whether all such earthquakes rupture the entire margin or just a segment of it. The calendar age range uncertainty of hundreds of years for accelerator mass spectrometry $^{14}C$ dating translates to a similar degree of uncertainty in dating plate-boundary earthquakes. Nonetheless, correlating earthquakes by age among coastal sites may indicate rupture extent for a few plate-boundary earthquakes. Another unresolved question is whether upper-plate faults can be triggered by plate-boundary earthquakes on the Cascadia margin (McInelly and Kelsey, 1990; Goldfinger et al., 1992; McNeill et al., 1998; Nelson et al., 1998).

We address several of these unresolved Cascadia seismicity questions with a 5500-yr-long record of plate-boundary earthquakes from the lower Sixes River valley in south coastal Oregon (Fig. 1). Our research has three objectives. The first is to collect and evaluate evidence for plate-boundary earthquakes in the stratigraphic record of buried wetland soils in the lower Sixes River valley. The second objective is to compare the times of plate-boundary earthquakes at the lower Sixes River

*E-mail: hmk1@axe.humboldt.edu.

*GSA Bulletin*; March 2002; v. 114; no. 3; p. 298–314; 12 figures; 7 tables; Data Repository item 2002038.

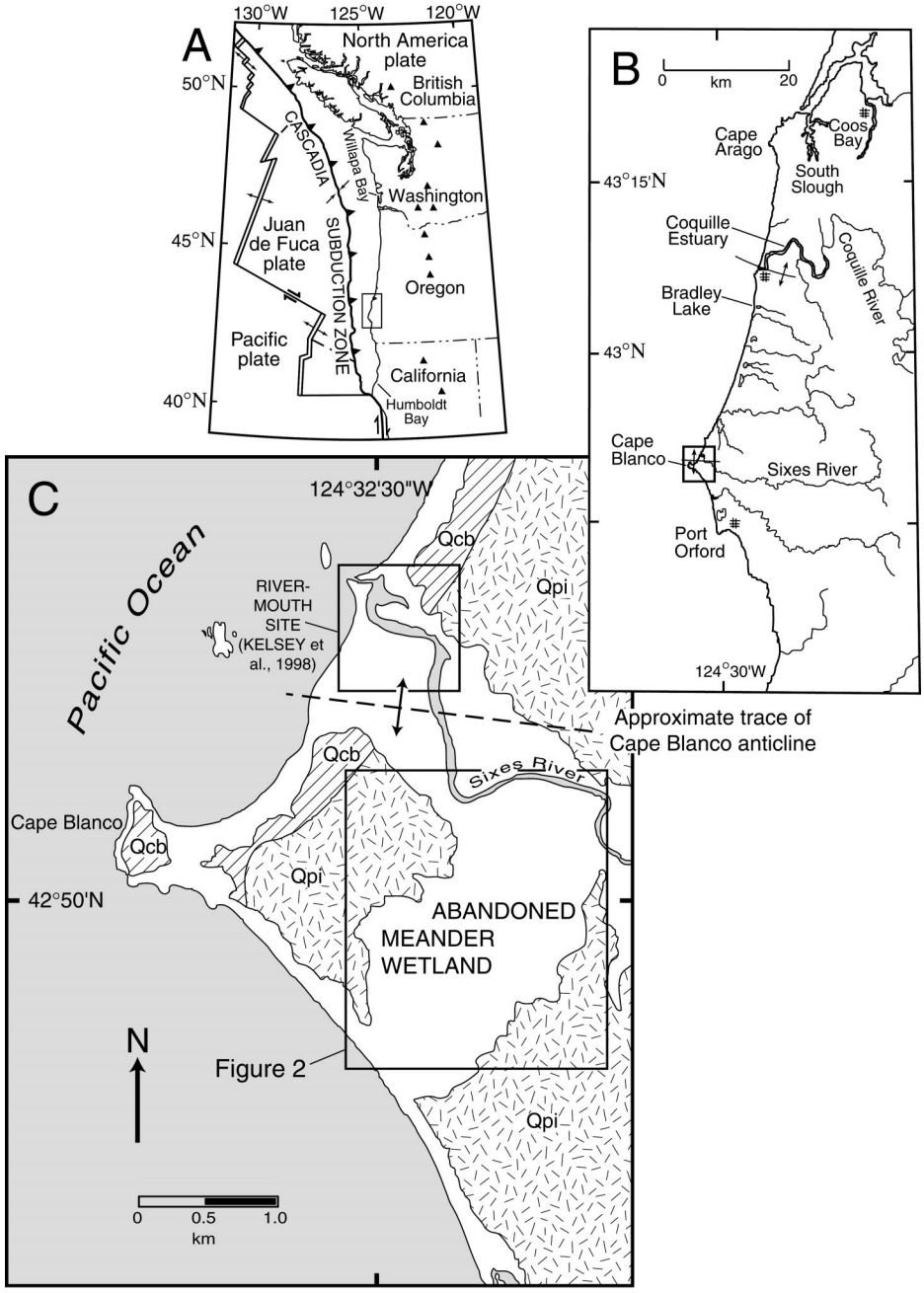


**Figure 1. (A) Plate-tectonic setting of southern coastal Oregon; triangles are volcanoes of the Cascade arc. (B) Location map of south coastal Oregon showing Cape Blanco, Sixes River, and other sites (Bradley Lake, Coquille estuary, Coos Bay) where paleoseismological studies have been carried out. (C) Map of lower Sixes River valley showing location of abandoned-meander wetland and the approximate trace of the Cape Blanco anticline (Kelsey, 1990). Also shown is the river-mouth site of Kelsey et al. (1998). Qcb and Qpi—upper Pleistocene terrace deposits of the Cape Blanco and Pioneer marine terraces (Kelsey, 1990). Area without pattern consists of hillslope and valley-bottom lands.**

valley with times of plate-boundary earthquakes elsewhere on the Cascadia subduction margin. By comparing earthquake histories at different locations on the margin, we evaluate whether some earthquakes are confined to just one segment of the margin. The upper-plate Cape Blanco anticline (Fig. 1) is a broad, 15-km-wavelength fold developed in deposits of the lower Sixes River that are of late Neogene to late Quaternary age (Kelsey, 1990). The third objective is to assess, by utilizing the lateral extent and variation in depth of buried soils perpendicular to the axis, whether the anticline has deformed during plate-boundary earthquakes.

## COASTAL SETTING OF THE LOWER SIXES RIVER VALLEY

The lower Sixes River valley is a freshwater lowland; tidal marshes do not occur in the lower valley because the estuary is confined to the active river channel and the valley lowlands are all higher than the elevation of mean higher high water (MHHW), which is 0.98 m relative to the National Geodetic Vertical Datum (NGVD). All reported elevations in the lower Sixes River valley are tied to the tidal datum at the Port Orford tide gauge, 11 km to the south (National Ocean Survey, 1977).

The present-day uplift rate in the lower Sixes River valley is 4–5 mm/yr (Mitchell et al., 1994). This uplift rate, for the approximate period 1930–1985, is inferred from 1970s to 1990s tide-gage records along the Oregon coast, including the Port Orford tide gage, and from repeated leveling surveys (1930s–1980s) along the coastal highway 6 km east of the lower Sixes valley (Mitchell et al., 1994). Mitchell et al. (1994) ascribed this exceptionally high rate of short-term uplift to strain accumulation above the locked part of the subduction zone. The 4–5 mm/yr uplift rate is 3–10 times greater than the long-term (~100 000 yr) permanent uplift rate for the Cape Blanco area based on marine-terrace studies, which is 0.5–1.2 m/k.y. (Kelsey, 1990).

Two areas of the lower Sixes River valley, the river-mouth area and the abandoned-meander wetland area (Fig. 1), provide stratigraphic data on late Holocene relative sea-level changes. At the river-mouth site, there is stratigraphic evidence for an abrupt relative sea-level rise and a tsunami ~300 yr ago (Kelsey et al., 1998), both probably generated by the A.D. 1700 Cascadia earthquake (Satake et al., 1996; Jacoby et al., 1997; Yamaguchi et al., 1997).

This paper focuses on an ~1.8 km$^2$ abandoned-meander wetland bordered by the Sixes River (Fig. 2). The wetland ranges in elevation from 1.7 to 4.2 m NGVD. The drier, northern part of the wetland is slightly higher (~5.5 m NGVD) because it is a natural levee built of Sixes River overbank deposits. The remainder of the abandoned meander is freshwater marsh and swamp, which drains to the north by an outlet through the levee (Fig. 2).

The meander valley was first incised and

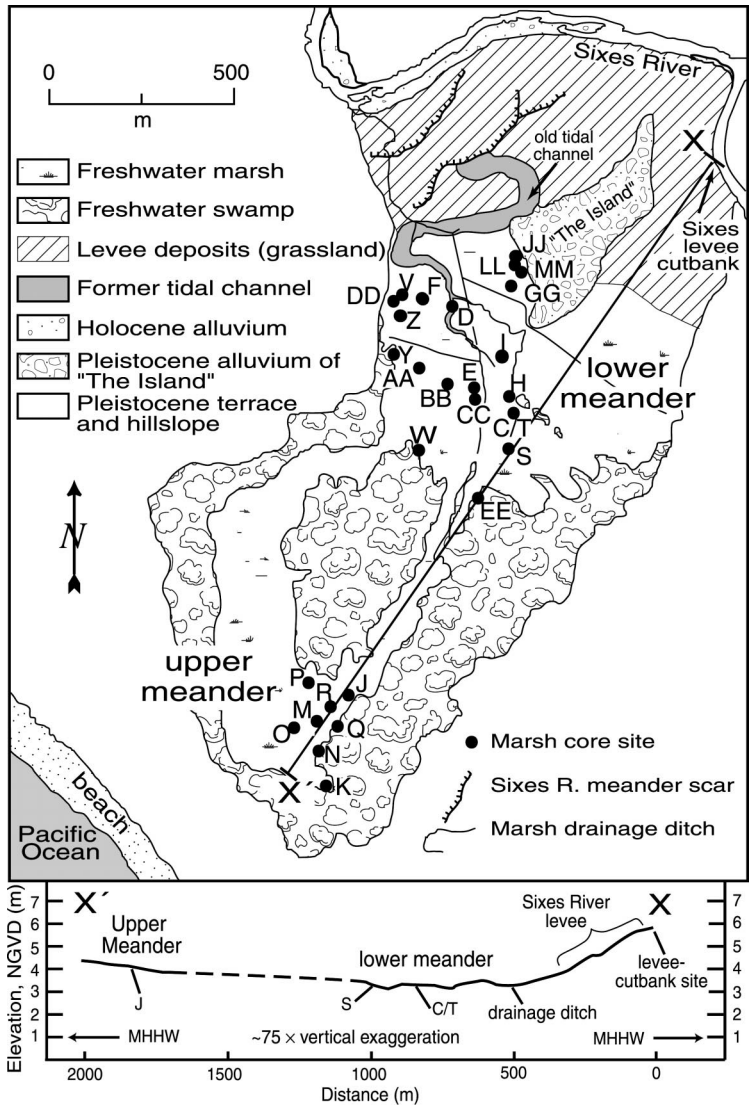


**Figure 2. Map of the abandoned-meander wetland in the lower Sixes River valley, showing the three study sites: upper meander, lower meander, and Sixes levee cutbank. Map shows all core sites from which subsurface stratigraphic data were collected. Topographic profile (bottom), constructed from survey points at 25 m spacing, has elevation accuracy of ±0.10 m. Dotted line on profile delineates extrapolated topography where surveying was not carried out. MHHW—mean higher high water (0.98 m above the NGVD [National Geodetic Vertical Datum]).**

then cut off when sea level was relatively lower in latest Pleistocene or early Holocene time. During the Holocene, the meander valley filled with fine-grained estuarine, tidal-marsh, and freshwater marsh sediments in response to sea-level rise. On the basis of cored samples, these sediments are at least 9 m thick and probably much thicker.

## APPROACH AND METHODS

We use three approaches to determine whether buried soils in the meander valley represent plate-boundary earthquakes. The approaches address criteria discussed by Nelson et al. (1996a) for inferring repeated coseismic subsidence of coastal wetland soils by plate-boundary earthquakes. The three approaches include detailed description of coastal wetland stratigraphy as revealed in outcrop or core, selection and $^{14}C$ dating of those organic materials that best indicate times of abrupt relative sea-level change that occasioned soil burial, and utilization of diatom biostratigraphy both to assess whether major shifts in salinity accompany abrupt changes stratigraphically upward from soil and mud and to estimate the magnitude of relative sea-level change associated with burial of individual wetland soils.

### Lithostratigraphic Investigations

Widespread sudden submergence of vegetated wetlands, tsunami deposits that accompany sudden submergence, and liquefied sediment are all lithostratigraphic evidence for plate-boundary earthquakes. If coseismic vertical changes in land level (~0.5–3.0 m) have occurred repeatedly in the late Holocene, coastal wetland sites that are in the elevation range of mean tide to mean higher high water should show concomitant widespread stratigraphic and ecologic changes indicative of repeated abrupt sea-level change (Atwater, 1987; Darienzo and Peterson, 1990; Nelson and Kashima, 1993; Darienzo et al., 1994; Guilbault et al., 1995; Hemphill-Haley, 1995; Nelson et al., 1996b; Atwater and Hemphill-Haley, 1997; Nelson et al., 1998). If tsunamis accompanied seismicity, sites within hundreds of meters of the coast and within 3–10 m of sea level should preserve continuous or discontinuous sheets of sand or sandy mud, transported landward by a tsunami (Bourgeois and Reinhart, 1989; Minoura and Nakaya, 1991; Clague and Bobrowsky, 1994; Dawson, 1994). Finally, if severe shaking occurred during subduction-related earthquakes, fine-grained, water-saturated sandy deposits might show evidence of liquefaction (Obermeier et al., 1985, 1990; Atwater, 1987; Clague et al., 1997; Obermeier and Dickenson, 2000).

One important aspect of the stratigraphic descriptions involved identifying buried soils, and we use the term ''soil'' to refer both to peaty O horizons of Histosols (Soil Survey Staff, 1998), in which organic content is >50% by volume, and A horizons of Inceptisols (Soil Survey Staff, 1998) in which organic content is <50% by volume. The term ''mud'' refers to silty-clay loam or silty clay. Both O and A horizons have roots of herbaceous plants, but roots are sparse or not present in the intervening mud. Whereas the contact separating soil from overlying mud is generally abrupt (<1–3 mm) or clear (3–10 mm), the transition from mud to overlying soil is generally gradational (>10 mm).

We investigated lithostratigraphy at three sites distributed over the abandoned-meander wetland (Fig. 2). These sites include the Sixes River levee-cutbank site at river km 3.6 (distance upstream along channel from river mouth), the lower-meander site, and the upper-meander site (Fig. 2). The Sixes levee cutbank is a small site (32-m-long cutbank exposure),

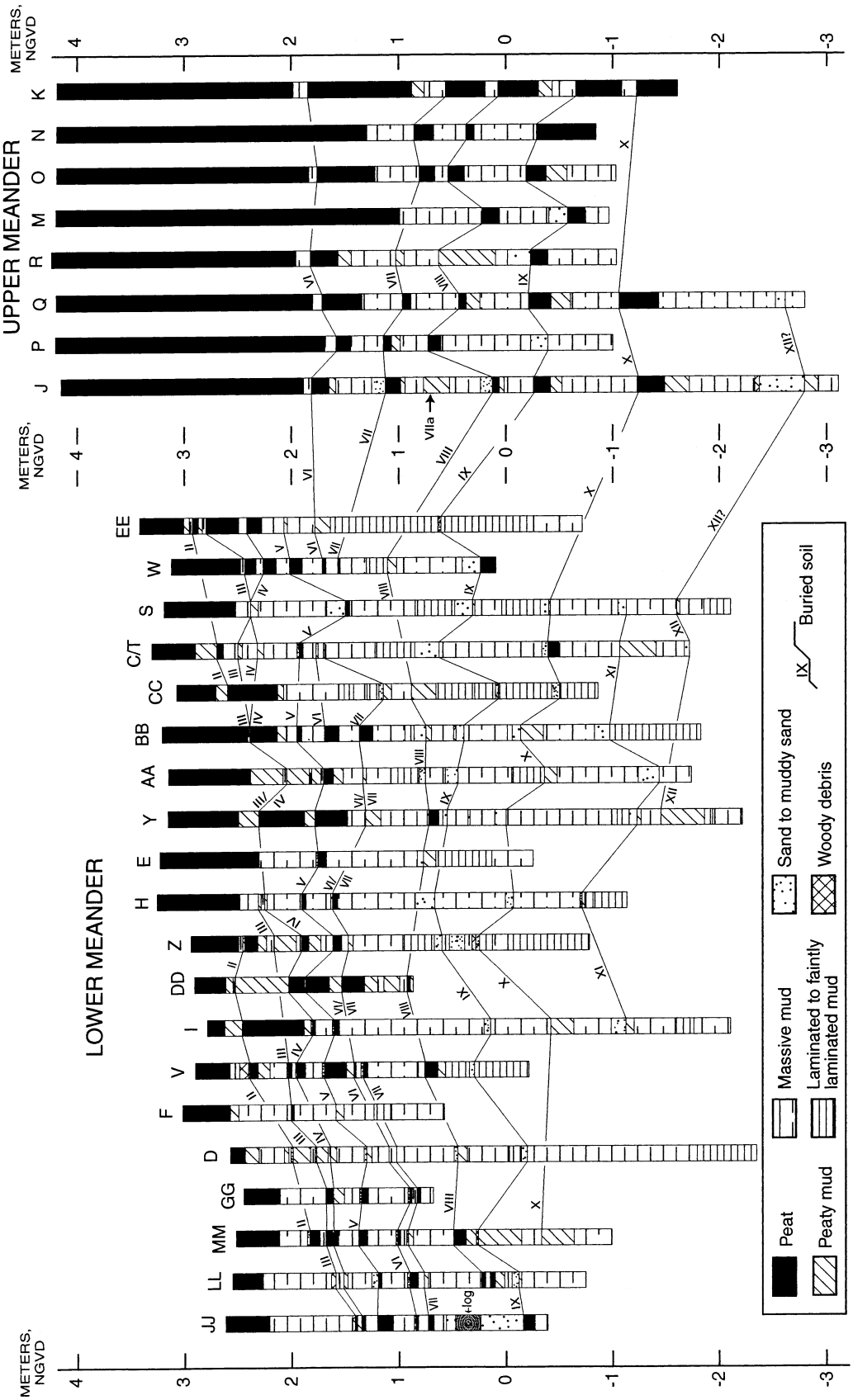


**Figure 3. Lithostratigraphy of 28 cores in the abandoned-meander wetland, ordered approximately from north to south across the wetland. Cores are positioned vertically on the basis of surveyed elevations, which are accurate to the nearest ±0.01 m. Eight core sites (K, M, N, O, P, Q, DD, and EE) were not surveyed. Elevations for these sites were estimated on the basis of the nearest surveyed site. Tie lines show correlations of buried soil horizons among cores.**

TABLE 1. ATTRIBUTES ASSOCIATED WITH BURIED SOILS, LOWER-MEANDER SITE, SIXES RIVER VALLEY

| Buried Soil number | Depth range to top of buried soil (cm) | Number of cores that sample buried soil | Abruptness of upper soil contact: abrupt-clear-gradual-not recorded* | Number of cores that sample sandy deposit overlying buried soil | Number of cores that sample sand deposit at stratigraphic level of buried soil but buried soil not present | Average thickness (cm) of sand associated with buried soil horizon ($n$ = number of sand layers) | Cores in which sand has multiple fining-upward cycles ($n$ = number of fining-upward cycles) |
|---|---|---|---|---|---|---|---|
| II | 20–65 | 9 | 1-3-1-4 | 4 | None | 3.3, $n = 4$ | None |
| III† | 70–110 | 11, (7)† | 4-3-4-7 | 1 or 2§ | None | 0.5, $n = 1$ | None |
| IV† | 80–130 | 11, (7)† | 9-2-2-5 | 1 or 2§ | None | 0.1, $n = 1$ | None |
| V | 110–160 | 20 | 13-2-1-2 | 9 | None | 3.4, $n = 9$ | S, $n = 3$ |
| VI† | 140–180 | 10, (6)† | 9-1-1-5 | 5 to 8# | None | 0.9, $n = 5$ | None |
| VII† | 150–190 | 10, (6)† | 6-1-3-6 | 2 to 5** | None | 0.8, $n = 2$ | None |
| VIII | 180–240 | 10 | 6-3-0-1 | 5 | 1 | 8.5, $n = 7$ | None |
| IX†† | 225–300 | 4†† | 4-0-0-0 | 2 | 13†† | 15.2, $n = 15$ | JJ, $n = 3$ |
| X | 270–380 | 6 | 3-3-0-0 | 4 | 4 | 16.5, $n = 8$ | None |
| XI | 390–470 | 4 | 3-0-1-0 | 3 | 3 | 7.5, $n = 4$ | None |
| XII§§ | 460–500 | 2§§ | 1-0-1-0 | None | 1§§ | 7.5, $n = 2$ | None |

*Number of contacts that are abrupt, clear, gradual or not recorded: abrupt: <1–3 mm; clear: >3–10 mm; gradual: >10 mm; not recorded: abruptness of contact not recorded either because core was logged quickly or core preservation was poor.

†Buried soils III and IV, and buried soils VI and VII, are buried soil couplets because for each set, the top of one soil is on average only 13–14 cm below the top of the successively higher soil (Table 3). Because of the close spacing, if one of the soils of the couplet is missing, it is not evident which one it is. Therefore, when accounting for the number of buried soils for soils II and IV, and for soils VI and VII, the number not in parentheses is the number of cores for which both buried soils are accounted for, and the number in parentheses is the number of cores for which either one or the other of the buried soil is accounted for but not both.

§For buried soil couplets III and IV, one core has a sandy deposit overlying both soils III and IV, and another core has a sandy deposit overlying either buried soil III or IV.

#For buried soil VI, five cores have a sandy deposit overlying VI; in an additional three cores, a sandy deposit overlies either buried soil VI or buried soil VII.

**For buried soil VII, two cores have a sandy deposit overlying VII; in an additional three cores, a sandy deposit overlies either buried soil VI or buried soil VII.

††Buried soil IX is observed in four cores; in an additional 13 cores, buried soil IX is represented by a clean, medium to fine sand resting on an abrupt erosional contact with no buried soil underlying the sand.

§§Buried soil XII is preserved in two cores as peat or a zone of concentrated roots and in one other core as clean, medium-fine sand.

whereas the lower-meander and upper-meander sites encompass larger areas (0.38 and 1.7 km$^2$, respectively) within a single abandoned meander. A topographic profile from the Sixes River levee-cutbank site southwest across the lower-meander site to the upper-meander site (Fig. 2) depicts the relative elevations of these sites. The upper- and lower-meander sites were investigated by using coring techniques; the levee-cutbank site was investigated in outcrop. We logged twenty-eight 2.5-cm-diameter gouge cores throughout the abandoned meander. These were supplemented by 7.5-cm-diameter cores at five of these sites. An additional twenty-one reconnaissance cores were quickly logged in order to identify optimal locations for core investigations.

## Radiocarbon Dating

Samples whose ages most closely represent the time at which a soil was buried by sand and/or mud were submitted for radiocarbon dating. Dated material primarily consisted of delicate woody detritus, seeds, and herbaceous stems and roots.

Delicate woody detritus was collected from woody ''trash'' layers or sands directly overlying buried soils and included leaf parts, small twigs with bark attached, and spruce needles. Seeds were collected either within the sandy deposit overlying a buried soil or within the upper 1 cm of the buried soil. We tried to

TABLE 2. ATTRIBUTES ASSOCIATED WITH BURIED SOILS, UPPER-MEANDER SITE, SIXES RIVER VALLEY

| Buried soil number | Depth range to top of buried soil (cm) | Number of cores that sample buried soil | Abruptness of upper soil contact* | Number of cores that sample sandy deposit overlying buried soil | Number of cores that sample sand deposit at stratigraphic level of buried soil but buried soil not present | Average thickness (cm) of sand associated with buried soil horizon ($n$ = number of sand layers) | Cores in which sand has multiple fining-upward cycles, ($n$ = number of cycles) |
|---|---|---|---|---|---|---|---|
| VI | 230–260 | 6 | Clear | None | None | N.A.† | None |
| VII | 305–363 | 7 | Abrupt | 1 | None | 10.2, $n = 1$ | None |
| VIIa§ | 335 | 1 | Abrupt | None | None | N.A.† | None |
| VIII | 350–420 | 8 | Abrupt | 1 | None | 5.3, $n = 1$ | J, $n = 2$ |
| IX# | 437–485 | 7 | Abrupt | 2 | 1 | 24.8, $n = 3$ | None |
| X | 526–538 | 3 | Abrupt | None | None | N.A.† | None |
| XII** | 695 | 1 | Clear | 1 | 1 | 25.0, $n = 2$ | J, $n = 5$ |

*Note*: In the upper meander, the core J site was cored and described on two separate occasions (1993; 1995), whereas the seven other cores (K, M, N, O, P, Q, R) were reconnaissance cores and have less detailed stratigraphic descriptions. The upper 2.3 m of the upper-meander site, corresponding in time to the interval of buried soils II–V in the lower meander site, is entirely fresh-water peat (Fig. 3). There are no buried soils in this interval because the site was too high to record relative sea-level changes.

*Contact abruptness is tabulated for core J only: abrupt: <1 mm–3 mm; clear: >3 mm–10 mm.

†N.A.—not applicable. No sandy deposit is observed to be associated with this buried soil.

§Buried soil VIIa is a faint buried soil observed only in core J. On the basis of diatom biostratigraphy, the soil records a negligible change in relative sea level. This buried soil is not correlative with any soil in the lower-meander site on the basis of lithostratigraphy or age.

#In the upper-meander site, buried soil IX occurs in seven out of eight cores; in contrast, in the lower-meander site, buried soil IX consists of sand with no accompanying buried soil in 13 out of 17 cases.

**Buried soil XII (694.5–706.5 cm depth) is a gray silty clay loam with ~5% organic component composed of horizontally layered peat. This weak soil is overlain by a 42-cm-thick sand that consists of five fining-upward cycles.

TABLE 3. BURIED SOILS IN UPPER- AND LOWER-MEANDER SITES: AVERAGE DEPTHS, AVERAGE ELEVATIONS, AND STRATIGRAPHIC SEPARATIONS

| Soil | Lower meander | | | | Upper meander | | | |
|---|---|---|---|---|---|---|---|---|
| | Number of core sites | Average depth (m)* | Average elevation (m, NGVD)† | Stratigraphic separation (m)§ | Number of core sites | Average depth (m)* | Average elevation (m, NGVD)† | Stratigraphic separation (m)§ |
| Ground soil | 14 | 0 | 3.06 | N.A. | | 0 | 4.15 | N.A. |
| II | 6 | 0.53 | 2.35 | 0.71 | N.S. | N.S. | N.S. | N.S. |
| III | 10 | 0.88 | 2.00 | 0.35 | N.S. | N.S. | N.S. | N.S. |
| IV | 10 | 1.01 | 1.87 | 0.13 | N.S. | N.S. | N.S. | N.S. |
| V | 17 | 1.32 | 1.62 | 0.25 | N.S. | N.S. | N.S. | N.S. |
| VI | 10 | 1.53 | 1.26 | 0.36 | 5 | 2.45 | 1.75 | N.A. |
| VII | 10 | 1.65 | 1.12 | 0.14 | 7 | 3.27 | 0.93 | 0.82 |
| VIII | 9 | 2.18 | 0.69 | 0.43 | 8 | 3.80 | 0.42 | 0.51 |
| IX | 14 | 2.66 | 0.28 | 0.41 | 7 | 4.52 | –0.31 | 0.73 |
| X | 8 | 3.34 | –0.36 | 0.64 | 3 | 5.34 | –1.16 | 0.85 |
| XI | 4 | 4.12 | –1.01 | 0.65 | 1# | 6.94# | –2.79# | # |
| XII | 3 | 4.79 | –1.58 | 0.57 | 1# | 6.94# | –2.79# | # |

*Note*: The number of core sites used to calculate average elevation of a specified soil is in some cases less than the number of core sites where a specified soil is observed (Table 1) because some core sites do not have surveyed elevations. N.S.—no soil; buried soils V and younger are not present at the upper-meander site.

*Average depth: average depth to top of buried soil.

†Elevations of buried soil determined by subtracting depth of top of buried soil from surface elevation at core site. All ground surface elevations determined by Total Station survey, accuracy to nearest 0.01 m, referenced by benchmark to National Geodetic Vertical Datum (NGVD).

§Difference between average elevation of top of soil and average elevation of top of next highest buried soil (m). N.A.—not applicable; a difference in elevation cannot be determined because the stratigraphically next highest soil horizon does not exist.

#In the upper-meander site, one core (J) records one buried soil older than soil X. We are uncertain whether this buried soil, which is at depth 6.94 m and at elevation −2.79 m, correlates to buried soil XI or XII in the lower-meander site, although we tentatively correlate it to soil XII.

collect seeds and delicate, identifiable woody debris that would be broken up by significant transport or significant time. In so doing, we attempted to minimize the time between death of the delicate woody detritus or seeds and the time at which this material was deposited.

Herbaceous stems and roots were collected when it appeared they were killed by deposition associated with soil burial. Candidate herbaceous samples included stems flattened on a soil/mud contact (e.g., Atwater and Yamaguchi, 1991).

We submitted $^{14}C$ samples incrementally over the course of 10 yr; in so doing, we determined that unreliable dates came from unidentifiable wood or bark fragments and from herbaceous roots or stems that were not clearly flattened on the top of a buried soil (see Data Repository materials[1] for more information on sample analysis). Therefore, in the latter 6 yr of $^{14}C$ sampling, we only collected delicate, identifiable woody detritus and seeds.

### Diatom Biostratigraphy and Relative Sea-Level Changes

We used diatoms to assess environments of deposition and magnitudes of sea-level change that accompanied the burial of soils. Diatoms were common in most of the core samples we examined. For each sample, we attempted to identify 100 diatoms recognizable to the species level. In some cases (19 out of 130 analyses), there were <100 recognizable diatoms; in these cases, our paleoenvironment inference was based on those diatom valves that could be identified.

By tracking changes in diatom assemblages across buried soil contacts, we used diatoms to assess relative sea-level changes at times when soils were buried (Nelson and Kashima, 1993; Hemphill-Haley, 1995). In one core, we undertook a qualitative biostratigraphic analysis of diatom-assemblage changes immediately above and below buried soil contacts in order to estimate the magnitude of relative sea-level rise that brought on the burial of the wetland soils. The analysis relies on the observation that, in tidal marshes, specific diatom associations are limited to defined elevation ranges relative to mean tidal level (Hemphill-Haley, 1995) (see footnote 1 concerning Data Repository materials). Therefore, diatoms are used to estimate the magnitude of elevation shift of mean tide level associated with burial of individual wetland soils. We constructed a relative sea-level curve for the lower Sixes River valley from the diatom-derived estimates of paleo–mean tide level in conjunction with depth of buried soils and $^{14}C$ age data.

[1]GSA Data Repository item 2002038, analysis of $^{14}C$ samples (part I) and diatom biostratigraphy and determination of paleo–mean tide levels (part II), is available on the Web at http://www.geosociety.org/pubs/ft2002.htm. Requests may also be sent to editing@geosociety.org.

## ABANDONED-MEANDER WETLAND

### Buried Soils

Buried soils II through XII could be correlated throughout the lower-meander wetland on the basis of depth, lithostratigraphy, and stratigraphic separation (Fig. 3). Not all buried soils are present in each of the 20 lower-meander cores, but six cores (D, V, W, BB, LL, MM) contain nearly complete sequences of 7–9 buried soils. Buried soils VI through X are preserved in the upper meander and can be correlated, on the basis of depth and lithostratigraphy, among most of the eight upper-meander cores (Fig. 3). Buried soil I is not observed in the abandoned-meander wetland; it occurs at the Sixes River mouth area (Kelsey et al., 1998) (Fig. 1C).

Contact abruptness at the top of buried soils is a qualitative indicator of the suddenness of submergence of a soil (Nelson et al., 1996a). In the majority of instances, 59 out of 91 observations (Tables 1 and 2), upper soil contacts in the abandoned-meander wetland are abrupt (<1 mm to 3 mm).

Distinct attributes of individual or sets of buried soils in the lower meander aided in identification and subsequent correlation. For instance, buried soil V occurred at ~130 cm depth in almost every core in the lower meander (Table 1). In addition, two couplets of buried soils (III and IV, and VI and VII) typically occur closer together than the other buried soils. Stratigraphic separation (vertical distance from top of one soil to top of the next) for each couplet was, on average, 13–14 cm, whereas the other buried soils were separated from adjacent buried soils by 25–70 cm (Table 3).

Although two buried soil couplets occur in the lower meander, neither couplet occurs in the upper meander (Table 3). Soil couplet III/IV is too young to be preserved in the upper meander, where the youngest buried soil is VI. Soils VI and VII are not unusually close together in the upper meander (Fig. 3, Table 3). In the section Folding of Cape Blanco Anticline During Plate-Boundary Earthquakes and Origin of Soil Couplets, we discuss a possible tectonic implication of the observed difference in stratigraphic separation between soils VI and VII in the upper- and lower-meander sites.

The deepest buried soils (XI and XII, Fig. 3) were identified in fewer cores in the lower meander because not all cores could be pushed beyond 4 m. Buried soil XI was found at four core sites in the lower meander in the 390–470-cm-depth range (Table 1). Only seven cores in the lower meander penetrated deep

TABLE 4. RADIOCARBON AGES, ABANDONED MEANDER, SIXES RIVER VALLEY

| Sample I.D.* | Laboratory I.D.† | Date§ | $\delta^{13}C$ | $^{14}C$ age# | Dated material |
|---|---|---|---|---|---|
| Sixes levee-cutbank site (river km 3.6) | | | | | |
| 90 A 90 | B 40002 | 10/90 | –25.0§ | 190 ± 50 | In situ spruce root |
| 96 A 90 | QL 4910 | 05/97 | –24.2 | 183 ± 13 | In situ spruce root, ring numbers 38–42 |
| 91 A 375 | B 47082 | 9/91 | –25.0§ | 2450 ± 80 | In situ ~6-mm-diameter woody roots |
| 93 A 355 | GX 19892 | 3/94 | –26.8 | 2499 ± 66 | In situ woody roots |
| Lower meander site, cores GG, JJ, and MM | | | | | |
| 96 GG 76 | GX 22923 | 4/97 | –26.2 | 2065 ± 45 | 8-mm-long twig |
| 96 GG 111 | GX 22924 | 4/97 | –24.9 | 2305 ± 45 | 6 cm long herb stem base or rhizome |
| 96 GG 153.5 | GX 22925 | 4/97 | –27.6 | 2885 ± 45 | ~170 *Carex* sp. seeds |
| 96 JJ 252.5 | GX 22946 | 7/97 | –26.8 | 3840 ± 50 | Spruce needles, spruce cone parts, seeds |
| 98 MM 66 | GX 25680 | 07/99 | –28.7 | modern | Spruce needle fragments, 2 seeds |
| 98 MM 91 | GX 25681 | 07/99 | –25.2 | 1250 ± 40 | Spruce cone part, seeds, 3 husks |
| 98 MM 158.5 | GX 25682 | 07/99 | –28.7 | 3240 ± 40 | Spruce needle fragments |
| 98 MM 224.5 | GX 25683 | 07/99 | –26.2 | 3780 ± 50 | Spruce needles, spruce cone parts, seeds |
| Lower meander site, cores D, C/T, and S | | | | | |
| 93 D 123 | GX 19888 | 3/94 | –28.2 | 1644 ± 68 | In situ herbaceous root or stem |
| 93 C/T 360 | GX 19887 | 3/94 | –28.7 | 4398 ± 70 | 3 small twigs; 11 bark fragments |
| 93 C/T 135.1 | AA 17182 | 8/95 | –30.7 | 565 ± 50 | Herbaceous fragments |
| 93 S 164 | GX 19891 | 3/94 | –28.3 | 1864 ± 69 | In situ herbaceous root or stem |
| 93 S 291 | GX 20200 | 10/94 | –27.6 | 3732 ± 89 | Herb stems flattened on contact |
| Lower-meander site, core V | | | | | |
| 94 V 78–84 | AA 17183 | 8/95 | –27.4 | 2070 ± 45 | Wood fragments, 1 seed |
| 94 V 125–126 | AA 17184 | 8/95 | –28.5 | 2820 ± 65 | Twig with bark |
| 94 V 155A | AA 17185 | 8/95 | –28.6 | 2200 ± 80 | Herb stems and/or roots |
| 94 V 155B | AA 17186 | 8/95 | –29.1 | 3175 ± 65 | Spruce needles |
| 94 V 209 | GX 20201 | 10/94 | –27.5 | 3546 ± 64 | 3 twig fragments, 2 with bark |
| 94 V 256 | GX 20202 | 10/94 | –28.3 | 3864 ± 63 | 6 spruce needles, 1 twig, 1 seed |
| Lower-meander site, core BB | | | | | |
| 95 BB 132.5 | GX 24243 | 7/98 | –26.3 | 2520 ± 40 | Seeds |
| 95 BB 158.5 | GX 23048 | 7/97 | –28.0 | 2880 ± 50 | Paper-like husks, one seed |
| 95 BB 189 | GX 23049 | 7/97 | –26.2 | 3240 ± 50 | Seeds |
| 94 BB 271.7 | AA 17178 | 9/95 | –27.4 | 5170 ± 60 | Unidentified wood fragments |
| 95 BB 276– | AA 19420 | 6/96 | –27.1 | 3875 ± 55 | One 1.5-mm-diameter twig with bark |
| 94 BB 404.4 | AA 17179 | 8/95 | –24.1 | 4630 ± 65 | 1 wood twig |
| Upper-meander site | | | | | |
| 95 J 71 ** | AA 19337 | 6/96 | –23.3 | 1545 ± 50 | 18 seeds |
| 95 J 141 ** | AA 19338 | 6/96 | –27.0 | 1905 ± 55 | 7 twigs with bark; 10–32 mm long. |
| 95 J 198 ** | AA 19339 | 6/96 | –23.4 | 2300 ± 50 | 35 seeds; >20 paper-like bud husks |
| 95 J 232 | AA 19340 | 6/96 | –28.3 | 2710 ± 55 | Bulk peat: 40% herb roots, 60% humified |
| 93 J 295 | GX 19889 | 3/94 | –28.0 | 2678 ± 73 | Herb stems entombed in very fine sand |
| 95 J 300 | GX 24243 | 7/98 | –29.4 | 3250 ± 40 | Seeds |
| 95 J 301 | GX 23045 | 7/97 | –29.6 | 3340 ± 50 | Spruce needles, seeds, leaf parts, moss |
| 93 J 335 | AA 17180 | 8/95 | –28.5 | 3045 ± 65 | Herb stem |
| 93 J 391 | GX 19890 | 3/94 | –27.4 | 3419 ± 67 | Spruce needles, twigs, cone part |
| 95 J 435 | GX 23046 | 7/97 | –26.8 | 3900 ± 40 | Seeds, one red husk |
| 93 J 441 | AA 17181 | 8/95 | –27.9 | 2665 ± 80 | Herb fragments |
| 93 J 537 | GX 20199 | 10/94 | –15.2 | 4319 ± 76 | 3 herb stems flattened on contact |
| 95 J 657.5 | AA 19421 | 6/96 | –25.5 | 5205 ± 65 | 40-mm-long, 2-mm-diameter twig |

*Sample code includes: year sampled; site designation (see Fig. 2); depth (cm) to top of sample.
†Laboratory prefixes and measurement methods: B, Beta Analytic, measurement by liquid scintillation, age calculated for an assumed fractionation ($\delta^{13}C$) of −25.0‰; QL, Quaternary Isotope Lab, University of Washington, high-precision proportional gas method; GX, Geochron Laboratories, accelerator mass spectrometry; AA, University of Arizona, accelerator mass spectrometry.
§Laboratory run date: month/year.
#Laboratory reported $^{14}C$ age (one standard deviation).
**Dated material from a massive peat section that is not associated with a specific buried soil.

enough (460–500 cm) potentially to reach buried soil XII; soil XII occurs at two of these sites (Fig. 3, Table 1).

Buried soils in the upper meander (Table 2) were correlated to soils in the lower meander on the basis of age because the ~500 m of uncored distance between the two sites (Fig. 2) precluded the use of depth and stratigraphic separation as a basis for correlation. Correlation was based mainly on two $^{14}C$ ages on the second buried soil in the upper meander (3250 ± 40 $^{14}C$ yr B.P., sample number 95 J 300; 3340 ± 50 $^{14}C$ yr B.P., 95 J 301; Table 4), which were an excellent match with three $^{14}C$ ages on buried soil VII in the lower meander (3175 ± 65 $^{14}C$ yr B.P., 94 V 155B; 3240 ± 50 $^{14}C$ yr B.P., 95 BB 189; 3240 ± 40 $^{14}C$ yr B.P., 98 MM 158.5; Table 4), On this basis, we interpreted the second buried soil in the upper meander to be soil VII. This correlation was confirmed by $^{14}C$ ages for two other buried soils (VIII and X) in core J from the upper meander that matched well with $^{14}C$ ages for correlative buried soils in cores V and C/T in the lower meander (Table 5). The interval of buried soils VI to X is ~120 cm deeper in the upper meander compared to the lower meander (Fig. 3) because buried soil VI in the upper meander is overlain by 245 cm of massive peat, whereas only ~140–160 cm of sediment bury soil VI in the lower meander (Fig. 3). On the basis of maps showing the lateral extent of preservation of each buried soil (Fig. 4), buried soils are extensively preserved in the abandoned-meander wetland, over an area at least as large as 200 000–420 000 $m^2$ (Table 5).

### Sandy Deposits Overlying Buried Soils

Sand or muddy sand deposits commonly overlie buried wetland soils on abrupt contacts (Tables 1 and 2). With the exception of buried soils III and IV, 50% or more of the buried soils in cores have an overlying sand deposit. Texture of the sand deposit ranges from medium-fine sand to sandy loam with up to 50% silt and clay.

Thicknesses of the sand deposits vary from <1 mm (several sand grains thick) to 42 cm. In general, the deeper-buried soils at both the upper- and lower-meander sites have thicker sand deposits (Tables 1 and 2). In the lower meander, sand deposits on soils II through VII are typically 0.5–3.0 cm thick, whereas those on soils VIII through XII are 7.5–16.5 cm thick on average. Because intermediate-depth buried soils (V, VI, and VII) are more likely to have sandy deposits overlying them than are the uppermost buried soils and because deeper buried soils (VIII and deeper) are more likely to be associated with thicker overlying sandy deposits (Tables 1 and 2), we infer that sand was more likely to enter the abandoned-meander wetland prior to the time of burial of soil V, ~2500 yr ago (Table 5).

Some cores penetrate a sand deposit at the expected stratigraphic level of deep soils (VIII and deeper), but the soil is absent (column 6, Table 1). For instance, buried soil IX occurs with an overlying sand deposit in four cores in the lower meander, but a sand deposit without accompanying buried soil IX is present in an additional 13 cores (Fig. 3, Table 1). In 11 out of 13 instances, the sand has an abrupt lower contact. The lower contact is erosional because the sand truncates laminations in the underlying mud substrate. In a few instances, the sand incorporates rip-up clasts derived from underlying strata.

Although most sandy deposits overlying buried soils are a single massive layer of sand or consist of one fining-upward bed, some of the thicker sand deposits have multiple fining-upward cycles (Tables 1 and 2; Fig. 5, core J, 395–402 and 652–694 cm depth). At 395–402

TABLE 5. AREAL EXTENT AND CALIBRATED $^{14}$C AGES FOR BURIED SOILS, UPPER- AND LOWER-MEANDER SITES

| Buried soil number | Extent of buried soil ($m^2$)* | $^{14}$C ages grouped by associated buried soil† (site designation) [sample composition]§ | Weighted mean ($^{14}$C age)# | Calibrated $^{14}$C age range** |
|---|---|---|---|---|
| II | 160 000 | | | |
| III (upper part of upper couplet) | 210 000 | 2065 ± 45 (GG) [DWD]<br>2070 ± 45 (V) [DWD] | 2068 ± 32 | 1940–2130 |
| IV (lower part of upper couplet) | 210 000 | | | |
| V | 300 000 | 2450 ± 80 (A) [DWD]<br>2499 ± 66 (A) [DWD]<br>2520 ± 40 (BB) [S] | 2505 ± 31 | 2460–2750 |
| VI (upper part of lower couplet) | 420 000 | 2880 ± 50 (BB) [S]<br>2885 ± 45 (GG) [S] | 2883 ± 33 | 2880–3160 |
| VII (lower part of lower couplet) | 420 000 | 3175 ± 65 (V) [DWD]<br>3240 ± 50 (BB) [S]<br>3240 ± 40 (MM) [DWD]<br>3250 ± 50 (J) [S]<br>3340 ± 50 (J) [DWD] | 3254 ± 22 | 3390–3560 |
| VIII | 420 000 | 3419 ± 67 (J) [DWD]<br>3546 ± 64 (V) [DWD] | 3486 ± 46 | 3630–3870 |
| IX | 420 000 | 3732 ± 89 (S) [HRS]<br>3780 ± 50 (MM) [DWD]<br>3864 ± 63 (V) [DWD]<br>3840 ± 50 (JJ) [DWD]<br>3875 ± 55 (BB) [DWD]<br>3900 ± 40 (J) [S] | 3849 ± 22 | 4150–4410 |
| X | 400 000 | 4362 ± 51 (J) [HRS]<br>4398 ± 70 (C/T) [DWD] | N.C.†† | 4830–5220 |
| XI | 220 000 | 4630 ± 65 (BB) [ DWD] | N.C.†† | 5050–5600 |
| XII | 220 000§§ | 5205 ± 65 (J) [DWD] | N.C.†† | 5750–6180 |

*Areal extent of buried soil horizon ($m^2$) in abandoned meander, as revealed in core and cutbank.

†$^{14}$C ages after removal of suspect ages (see text and see footnote 1 regarding Data Repository).

§DWD—delicate woody detritus; HRS—herbaceous roots and/or stems; S—seeds; stratigraphic position of samples is either in top of buried soil or in directly overlying sand deposit (see text).

#Weighted means are calculated for samples that, on the basis of chi square test, are statistically equivalent at the 95% level (Ward and Wilson, 1978); weighted means computed with $^{14}$C age calibration program (Calib version 4.3) of Stuiver et al. (1998).

**Calibrated years before A.D. 1950, using calibration program (Calib version 4.3) of Stuiver et al. (1998). Calibration incorporates two standard deviations and an error multiplier of one.

††N.C.—not calculated. No weighted mean is calculated because sample size is one.

§§Radiocarbon age 5205 ± 65 yr B.P. comes from the deepest buried soil at core J in the upper-meander site. We infer that this age is associated with buried soil XII in the lower-meander site; therefore, the lateral extent of soil XII is 220 000 $m^2$.

cm, two fining-upward sequences overlie buried soil VIII. The contact at the base of both fining-upward sequences is abrupt, whereas the top of the upper sequence is gradual. At 652–694 cm, five fining-upward sandy sequences overlie a peaty mud correlated to buried soil XII, and the texture of the individual fining-upward sequences varies (Fig. 5).

On the basis of the distribution and character of sandy deposits associated with buried soils, we infer that deposition of sand immediately followed the event responsible for burying the soil. Because sand abruptly overlies each buried soil but coverage of the soil by the sand is patchy, we infer that sand deposits are discontinuous sheets. The sand texture is clean and well sorted in most cases, and therefore we infer that the source was the beach or nearshore. Sand deposits also contain marine diatoms (see following section). If the sand comes from the beach, then the greatest inferred transport distance, from the river-mouth to upper-meander core sites, is ~3600 m. Because (1) the base of the sandy deposits usually is abrupt, (2) the bases of individual fining-upward sequences in a multiple fining-upward sediment sequence are abrupt, and (3) no soil occurs on top of any of the individual pulses, we conclude that single massive or fining-upward sand beds and multiple fining-upward sequences both are deposited rapidly, probably in minutes to hours. Finally, because at some sites within the abandoned meander, sandy deposits occur at levels of buried soils even though the buried soils are not preserved, we infer that sand was delivered both to those parts of the paleowetland with wetland soils and to those parts of the paleowetland either without a vegetated surface or where the vegetated surface had been eroded just prior to sand deposition.

### Diatom Biostratigraphy

On the basis of the number of freshwater diatom species versus the number of brackish and/or marine diatom species at different depths in one core each from the upper meander and lower meander (Fig. 6), we infer that, over an ~3000 yr transition period, site conditions changed at both core sites from permanently brackish and/or marine conditions to permanently fresh water (Fig. 6).

During the 3000-yr transition period, diatom populations fluctuated back and forth from brackish and/or marine species to freshwater species. This fluctuation in relative sea level was associated with the burial of wetland soils (Fig. 6). Core J shows that three major paleoecologic changes occurred in the period when the marsh was predominantly brackish and/or marine, each involving a change to freshwater conditions and then an abrupt shift back to brackish and/or marine conditions (Fig. 6). The change to fresh water (emergence) corresponds with the development of soils X, IX, and VII. Each abrupt shift back to brackish and/or marine conditions (abrupt submergence) corresponds to the abrupt burial of a soil by mud (Fig. 6). The mud immediately above buried soil VI records a brief, final shift to more brackish and/or marine conditions before core site J became a permanently freshwater marsh.

In core V, there are also four major paleoecologic changes from brackish and/or marine to freshwater conditions followed by abrupt shifts back to brackish and/or marine conditions. These changes correspond to the deposition of, and the subsequent burial of, soils VIII, VII, VI, and V (Fig. 6). Because sandy sediment that overlies buried soils contains brackish and/or marine diatoms (Fig. 6), we interpret that the same sediment-laden flows that transport sand also transport brackish and/or marine diatoms onto freshwater marsh soils at the outset of several of the instances of soil burial.

Combining observations from cores V and J, a shift to more freshwater conditions followed by an abrupt return to brackish and/or marine conditions characterizes soils X, IX, VIII, VII, VI, and V. For buried soil VIII, there is no evidence for paleoecologic change in core J, but there is for core V (Fig. 6).

The general history of relative sea level, constructed from calibrated age data for buried soils (Table 5) and from diatom-derived estimates of paleo–mean tide level (see footnote 1 for information on Data Repository items), is a rise from ca. 5.5 ka to 3.0 ka and a slight fall from ca. 3.0 ka to present (Fig. 7). The marsh at the core J site accreted to keep up with sea-level rise from 6.0 ka to ca. 3.0 ka (dashed line, Fig. 7). The marsh became emergent after ca. 3.0 ka because it con-

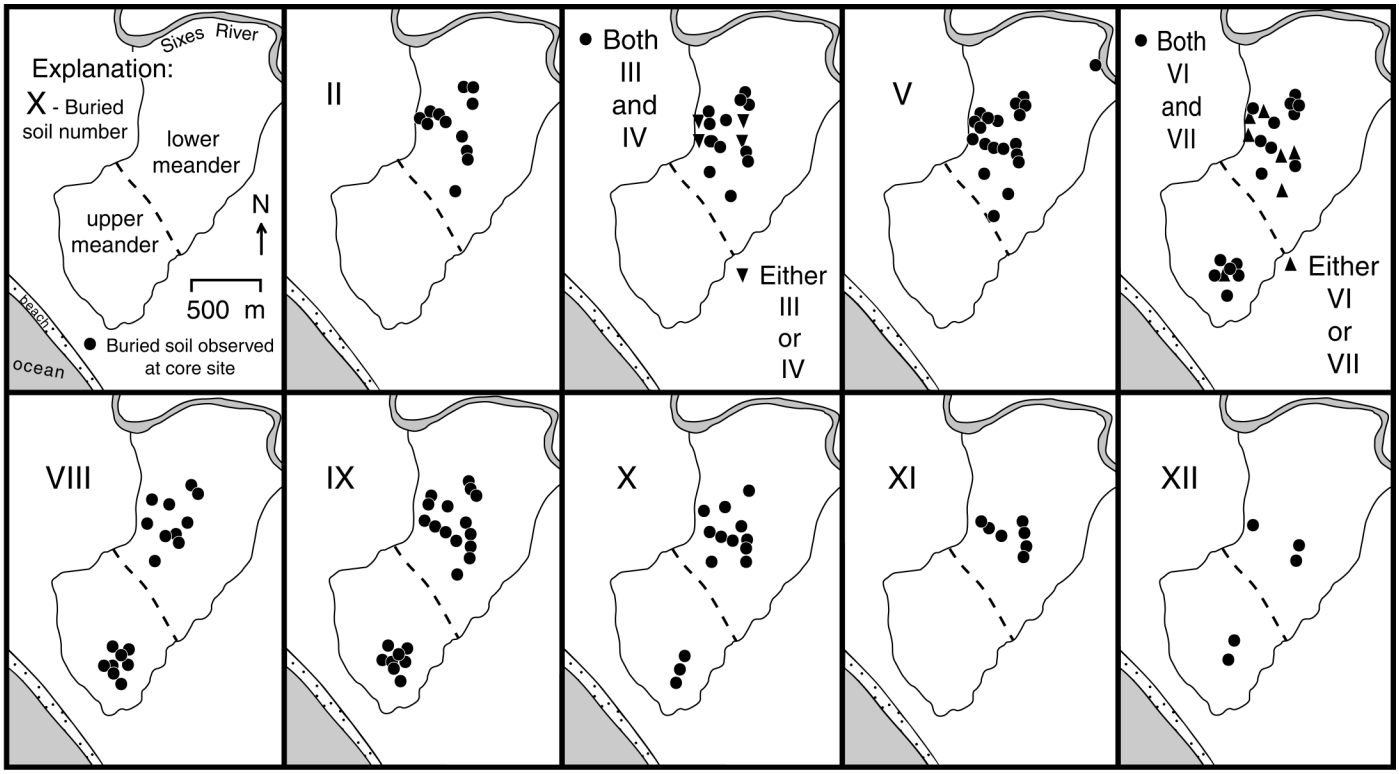


**Figure 4. Maps of the abandoned-meander wetland showing cores in which a specified buried soil (roman numerals) is preserved. Also shown are cores that sample a sand deposit at the stratigraphic level of the buried soil but the buried soil is not present. Preservation of buried soils III and IV, and of buried soils VI and VII, is shown on the same map because at some core sites, only one of two soils is preserved and it is not possible to identify which of the two buried soils is missing.**

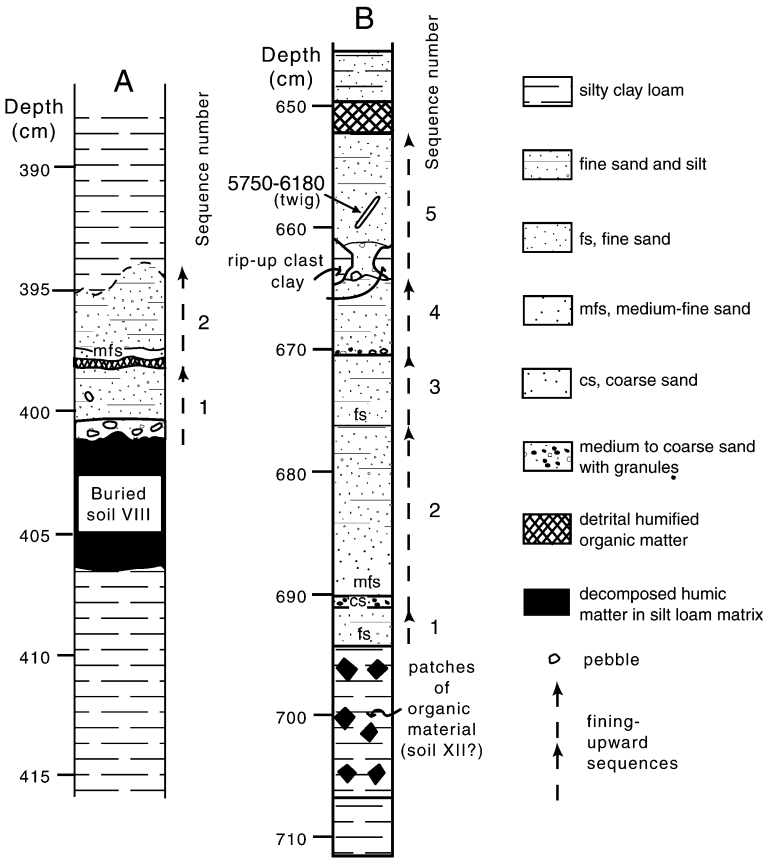


**Figure 5. Sketch of two intervals in core J showing repeated fining-upward sequences within a sandy deposit. (A) Two fining-upward sequences overlying buried soil VIII. (B) Five fining-upward sequences overlying an organic-rich silty-clay loam that we infer is correlative to buried soil XII in the lower meander. The coarse base of the highest sequence (fining-upward sequence 5) consists of medium sand, pebbles up to 6 mm across, and clay rip-up clasts up to 50 mm across. Depths are depth below ground surface. Calibrated radiocarbon age range in years before A.D. 1950 has 2σ uncertainty.**

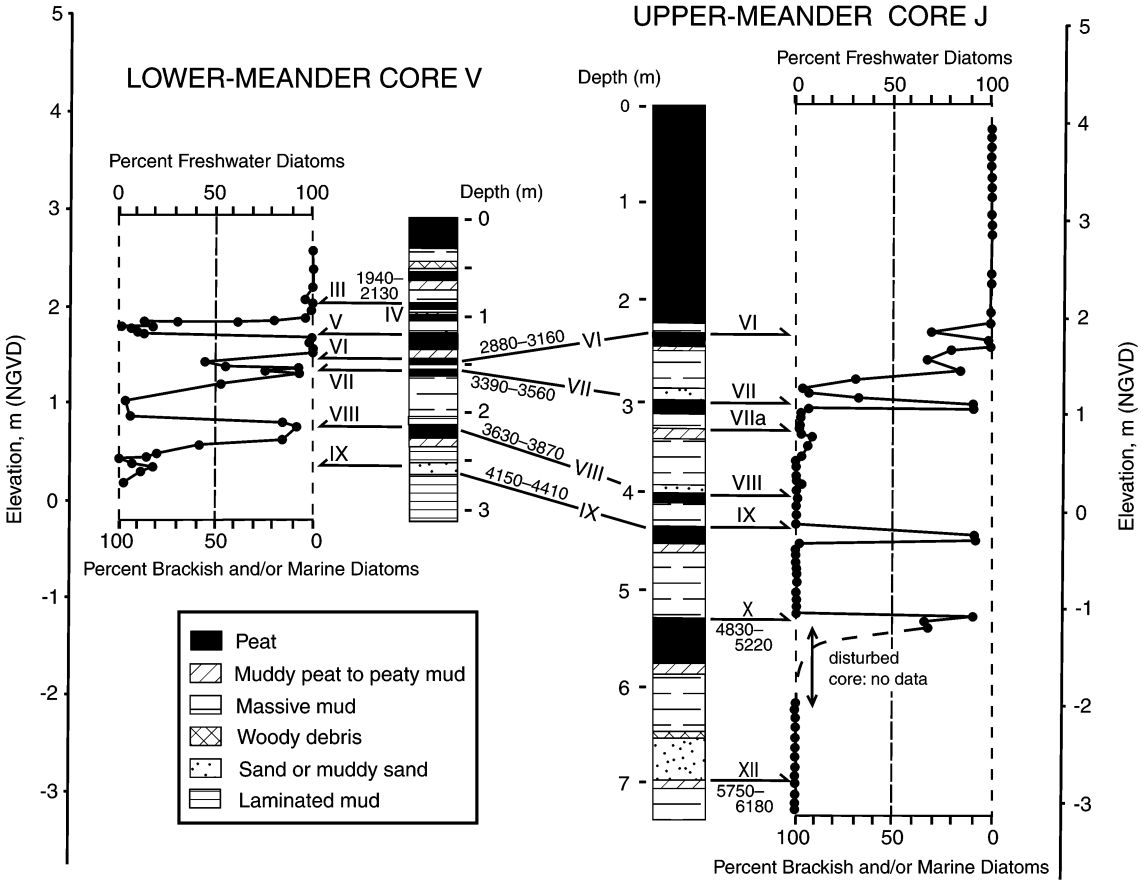


**Figure 6. Diatom biostratigraphy of cores V and J. Graphs show percent freshwater diatoms vs. percent brackish and/or marine diatoms as a function of depth in each core. Tie lines delineate correlative buried soils. In general, a transition upward from mud to peat is occasioned by a gradual change to more freshwater conditions, and an abrupt transition from peat stratigraphically upward to mud is accompanied by an abrupt transition to brackish and/or marine conditions. Calibrated radiocarbon age ranges in years before A.D. 1950 (2σ uncertainty) are based on $^{14}C$ ages in Table 5.**

TABLE 6. ESTIMATES OF PALEO–MEAN TIDE LEVEL (MTL) BEFORE AND AFTER SUBMERGENCE OF SOILS, CORE J, UPPER MEANDER

| Buried soil | Elevation (NGVD) soil/mud contact (m)* | Elevation (NGVD), diatom sample (m) | Paleoenvironment of diatom sample (bs)—before submergence (as)—after submergence | Vertical position of diatom sample relative to paleo-MTL (m)† | Elevation (NGVD), paleo-MTL (m)§ | Median submergence (m)# | Maximum/ minimum submergence (m)** |
|---|---|---|---|---|---|---|---|
| VI | 1.82 | 1.84 | Tidal flat (bs) | –0.2 to 0.8 | 2.04 to 1.04 | 1.4 | 2.4/0.4 |
| | | 1.81 | Fresh-water marsh (as) | 1.2 to 2.2 | 0.61 to −0.39 | | |
| VII | 1.12 | 1.14 | Tidal flat (bs) | –0.2 to 0.8 | 1.34 to 0.34 | 1.4 | 2.4/0.4 |
| | | 1.11 | Fresh-water marsh (as) | 1.2 to 2.2 | –0.09 to −1.09 | | |
| VIIa | 0.83 | 0.85 | High marsh (bs) | 0.8 to 1.4 | –0.05 to −0.55 | 0.0 | 0.6/NA |
| | | 0.82 | High marsh (as) | 0.8 to 1.4 | –0.02 to −0.58 | | |
| VIII | 0.14 | 0.15 | Tidal flat (bs) | –0.2 to 0.8 | 0.35 to −0.65 | 0.5 | 1.4/ NA |
| | | 0.13 | Low marsh (as) | 0.4 to 1.2 | –0.27 to −1.07 | | |
| IX | –0.20 | –0.19 | Tidal flat (bs) | –0.2 to 0.8 | 0.01 to −0.99 | 1.4 | 2.4/0.4 |
| | | –0.25 | Fresh-water marsh (as) | 1.2 to 2.2 | –1.45 to −2.45 | | |
| X | –1.05 | –1.06 | Tidal flat (bs) | –0.2 to 0.8 | –0.86 to −1.86 | 1.4 | 2.4/0.4 |
| | | –1.09 | Fresh-water marsh (as) | 1.2 to 2.2 | –2.29 to −3.29 | | |

*Soil/mud contact elevations depicted in Figure 3, core J.

†Elevation ranges for marsh and tide flat environments, relative to tidal datum, are depicted in Data Repository (see footnote 1) and Hemphill-Haley (1995). In order to avoid unnecessarily large upper bound to maximum submergence, we assign an upper elevation limit to the fresh-water marsh ecological zone and a lower elevation limit to the tidal-flat ecological zone such that the elevation range of these zones are both 1.0 m.

§Paleo–mean tide level elevations in this column are depicted in relative sea-level curve in Figure 7.

#Median elevation of MTL before submergence minus median elevation of MTL after submergence.

**See Figure 7. Minimum submergence is not applicable (NA) for soils VIIa and VIII because minimum submergence would be negative (indicating emergence), which is not possible for a stratigraphic transition upward from soil to mud.

tinued to accrete while relative sea level started to fall (Fig. 7).

Superimposed on the trend of relative sea-level rise followed by relative sea-level fall are five instances of abrupt relative sea-level rise (Fig. 7). The magnitude of submergence for soils X, IX, VIII, VII, and VI, reflected by diatom-assemblage changes across abrupt buried soil contacts, ranged from 0.5 to 2.4 m (median and maximum submergence, Table 6). We infer that submergence exceeded minimum estimates (Table 6; Fig. 7). In the case of soil VIII, minimum submergence is negative, indicating emergence (Fig. 7), and emergence is impossible given

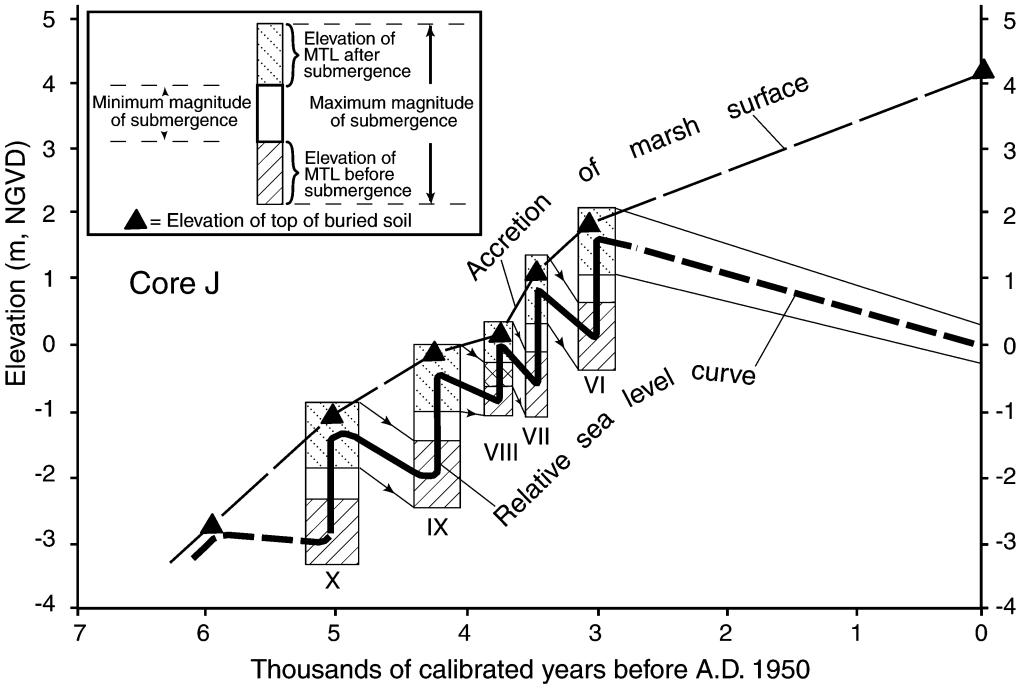


**Figure 7. Elevation of mean tidal level (MTL) over time ("relative sea-level curve") for core J, upper-meander site. Range of mean tidal level for buried soils VI through X is denoted by rectangles. Width of rectangles delineates estimated age range for the time of soil burial on the basis of radiocarbon age data (Table 5). Height of rectangles shows extent of abrupt rises in MTL associated with coseismic subsidence during subduction-zone–related earthquakes. Estimates of MTL paleoelevations (Table 6) were determined from fossil diatom assemblages (Hemphill-Haley, 1995) (see footnote 1 for material in Data Repository), and the envelope to the sea-level curve incorporates error related to estimating MTL from diatoms. Bold solid and dashed lines delineate best estimate of relative sea-level curve; curve is dashed from 3000 yr to present because of lack of buried soil record at core J in this time interval. Triangles mark elevations of top of individual buried soils in core J, and slope of dashed line depicts marsh-accretion rate ("accretion of marsh surface"). The lack of sensitivity of the site to relative sea-level change in the 3000 yr B.P. to present range (dashed bold line) is indicated by the observation that the marsh surface aggraded ~2.5 m from 3000 yr to the present at the same time that relative sea level dropped ~1.5 m.**

the biostratigraphic transition from soil to tidal mud.

### Age Assignments for Buried Soils

On the basis of the correlation of buried soils throughout the abandoned meander, $^{14}C$ age determinations for soils in individual cores (Table 4) were sorted into 1 of 11 buried soils (soils II–XII, Table 5). Radiocarbon ages from bulk peats (one age), unidentified wood fragments (two ages), and herb roots that were not flattened on a contact (nine ages) were eliminated prior to sorting ages (see footnote 1 for information concerning the Data Repository).

A best estimated age range for a particular buried soil depends on the number of $^{14}C$ ages available. Two buried soils, II and IV, have no $^{14}C$ age. Therefore, the best age estimate for these buried soils was made from bracketing ages from the next higher and the next lower buried soil (Table 5). Another two buried soils, XI and XII, which are the two oldest and deepest buried soils, have only one $^{14}C$ age each. This $^{14}C$ age, when calibrated to a calendar age range, is the best estimated age range for the buried soil (Table 5). Seven buried soils (II, V, VI, VII, VIII, IX, and X) have two or more $^{14}C$ ages. For these seven soils, we performed a chi square test of whether the $^{14}C$ ages are statistically equivalent at the 95% level. Because all seven groups of $^{14}C$ ages met the criteria of statistical equivalence, a weighted mean $^{14}C$ age was calculated (Ward and Wilson, 1978), and the weighted mean $^{14}C$ age was converted to a calibrated age range by using procedures of Stuiver et al. (1998) (Table 5).

Calibrated ages for buried soils VI and older do not overlap except for soils X and XI (Fig. 8; Table 5). The age assignments are

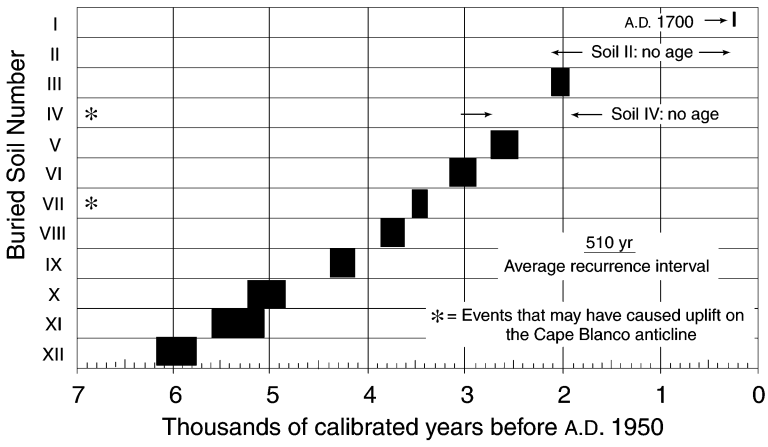


**Figure 8. Calibrated $^{14}C$ age ranges for Sixes River valley buried soils. The horizontal bars are graphical depictions of the calibrated age ranges in Table 5. Calibration (Calib version 4.3 of Stuiver et al., 1998) incorporates two standard deviations and an error multiplier of one.**

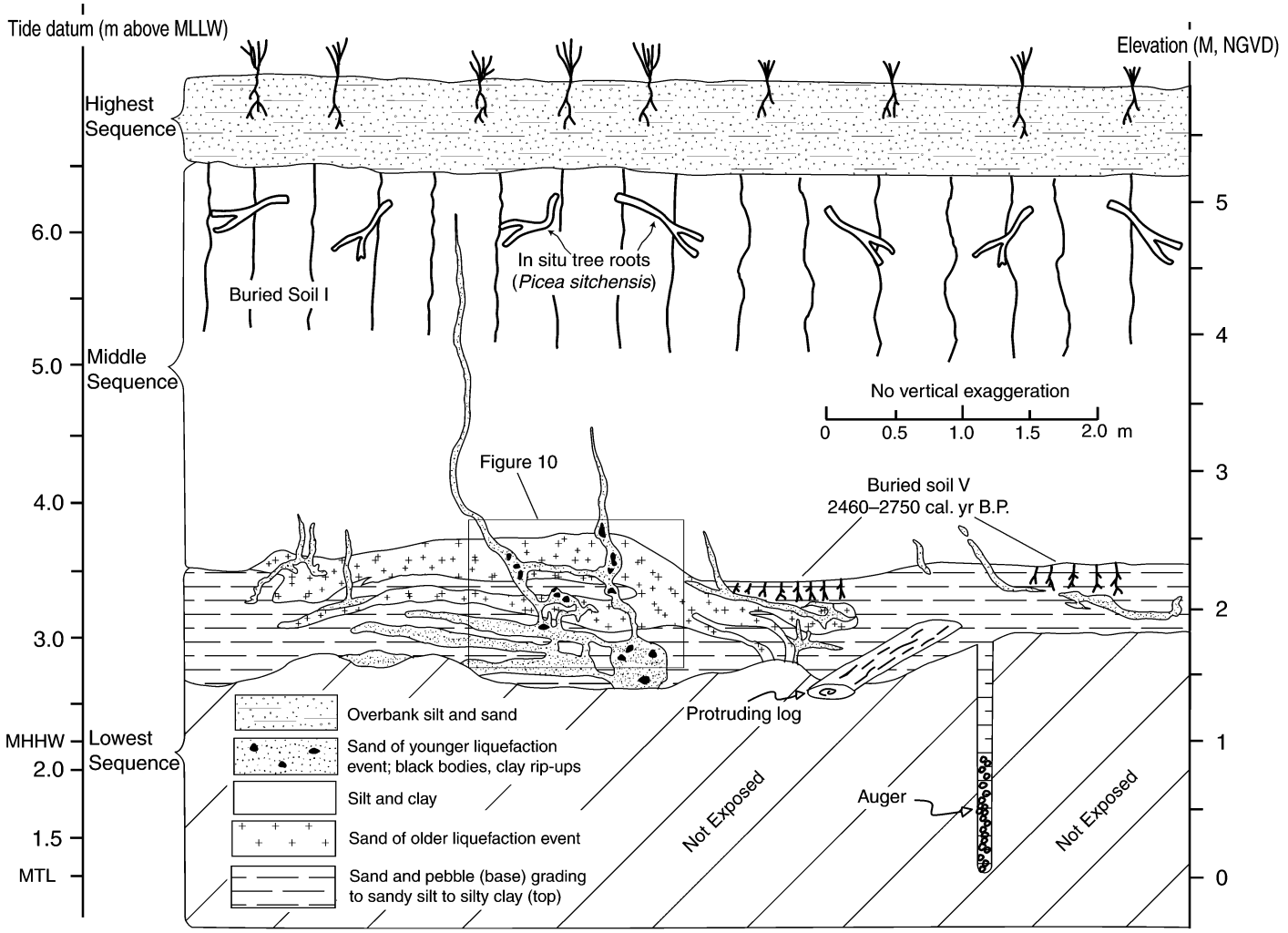


**Figure 9. Sketch of a part of the exposure at the cutbank site at river km 3.6. The sketch shows two instances of liquefaction within the estuarine deposits of late Holocene age in the lower Sixes River valley. About 2500 yr ago (approximate age of buried soil V, Table 5), liquefied sand vented onto a vegetated surface, forming a sand volcano. About 300 yr ago, liquefied sand intruded the first liquefaction feature and then intruded up into a silty clay unit that overlies the first liquefied sand unit. See text and Figure 10 for more details. Tree roots in buried soil I were killed after A.D. 1707 but before A.D. 1850; see Kelsey et al. (1998). MLLW—mean lower low water.**

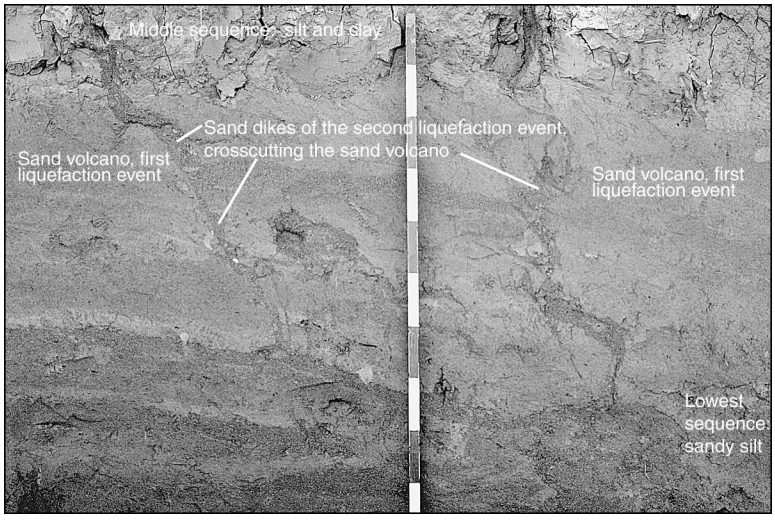


**Figure 10. Photograph showing detailed view of the liquefaction features depicted in Figure 9. Intervals on wooden staff are 0.1 m. The smooth-textured silty clay at the top of the photograph is the base of the middle sedimentary sequence. Most of the rest of the photograph shows two sand units representing two liquefaction events. The coarser grained sand, which includes both the three horizontal layers in the lower left and the two veins that rise from them, is sand of the second liquefaction event. This sand intrudes the sand of the older liquefaction event, which occurs in the middle part of the photograph. The older sand, which is not as well sorted as the younger sand, is part of a sand volcano that vented onto a paleo–ground surface (Fig. 9).**

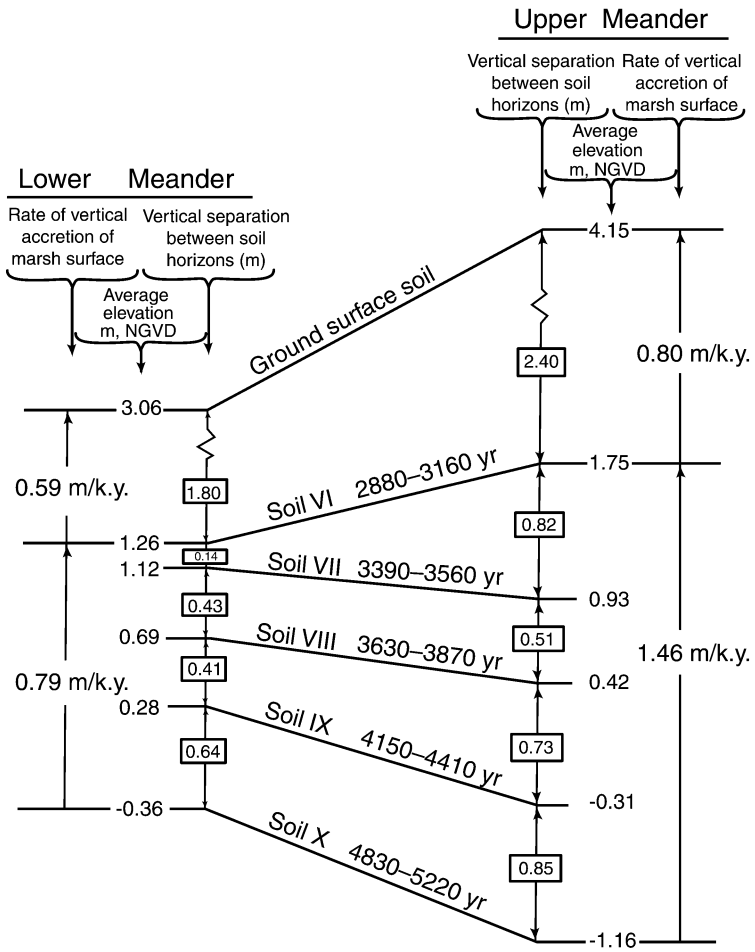


**Figure 11. Comparison of the stratigraphic separation of buried soils in the lower- and upper-meander sites. Figure also shows comparative rates of marsh surface accretion, on the basis of average depths to buried soils (Table 3) and $^{14}$C ages of soils (Table 5). Comparative accretion rates and vertical separations support the hypothesis, discussed in text, that during at least two plate-boundary earthquakes (one of which occurred ~3500 yr ago), folding in the upper plate resulted in more subsidence in the upper than in the lower meander. Calibrated radiocarbon ages (2σ uncertainty) are from weighted mean $^{14}$C ages (see Table 5).**

maximum ages, meaning the age of the buried soil may be younger but is no older than the assigned calibrated age. There is no age for soils II and IV; however, their ages must overlap the ages of underlying and overlying soils (Fig. 8).

## LEVEE-CUTBANK SITE

Alluvial and overbank sediment exposed at the Sixes River levee-cutbank site (Fig. 2) provides stratigraphic data that complement the data collected from cores in the upper- and lower-meander sites. Cutbank stratigraphy consists of three sedimentary sequences. These sequences were documented by logging a 5 m × 32 m cutbank exposure, a portion of which is shown in Figure 9. The lower two sequences are each capped by a buried soil.

### Buried Soils

The lowest sequence consists of an alluvial sand and sandy gravel at least 1 m thick that fines upward to a massive silt loam to silty-clay loam. A weak buried soil characterized by in situ roots of woody plants is developed on the upper part of the sequence. On the basis of two $^{14}$C ages on the roots (samples 91 A 375 and 93 A 355, Table 4), woody plants grew in this horizon ~2500 yr ago (Fig. 9). On the basis of $^{14}$C age, we infer that this lower buried soil at the levee-cutbank site correlates with buried soil V, the most extensively preserved buried soil in the lower meander (Table 5, Fig. 4). The next sequence is in clear (3–10 mm) contact above the buried soil of the lowest sequence.

The 2.5-m-thick middle sequence is a massive and homogeneous silty-clay loam to silty clay with root mottles throughout. A paleosol (buried soil I, Fig. 9) with distinctive subangular blocky structure and pedogenetically induced texture changes has formed in the upper 1.2 m. In situ spruce tree roots are preserved at the top of the paleosol. A high-precision $^{14}$C age (sample 96 A 90, Table 4) on one root indicates that the roots died either 100–172 yr or 224–243 yr before A.D. 1950 (discussion of this age summarized in Kelsey et al., 1998). Kelsey et al. (1998) correlated the buried soil on top of the middle sequence to the buried soil at the Sixes River mouth (buried soil I), which they inferred coseismically subsided and became inundated by a tsunami at the time of the A.D. 1700 Cascadia earthquake.

The highest sequence at the Cutbank site (Fig. 9) abruptly overlies the middle sequence. It consists of alluvial overbank deposits that buried the middle sequence after coastal subsidence in A.D. 1700 (Kelsey et al., 1998).

### Liquefaction Features at the Levee-Cutbank Site

Two sand bodies intrude strata at the levee-cutbank site. The older sand intrudes through the lowest sedimentary sequence and is deposited as a lensoid body on top of the lower buried soil (Fig. 9). The sand lens is thickest near the sand dikes that feed the lens and thins away from the feeder dikes (Fig. 9). The stratigraphic configuration of this liquefaction feature, in which a sand lens, fed by dikes, is extruded onto a soil, is similar to liquefaction sand blows described by Clague et al. (1997) that were extruded ~1700 yr ago onto a vegetated wetland surface on the Fraser River delta in southern British Columbia.

Because the lens of sand that spreads horizontally over the lower buried soil has the mounded appearance of a vented sand volcano and is thickest nearest the source dike (Fig. 9), we infer that it was extruded onto the surface rather than intruded as a sill. Extrusion of liquefied sand onto the lower buried soil was followed by soil burial. Had significant time elapsed (years) between venting of the sand and soil burial, roots and a paleosol probably would be preserved at the top of the lensoid sand. Because no soil is preserved, the sand body likely was buried by sediment deposited out of standing water shortly after the sand was extruded.

The second instance of sand fluidization in-

TABLE 7. CANDIDATE PALEOSEISMIC EVENTS AT THE SIXES RIVER: CALIBRATED AGE RANGE AND EVIDENCE FOR COSEISMIC SUBSIDENCE

| Candidate Paleo–seismic event (same number as correlative buried soil) | Calibrated age range* (yr before A.D. 1950) | Evidence for coseismic subsidence† | | | | | |
|---|---|---|---|---|---|---|---|
| | | Abrupt soil/mud contact (Tables 1 and 2) | Permanence of relative sea-level rise (>10 cm of tidal mud overlies buried soil) (Table 3) | Is lateral extent of soil/mud contact >150 000 m²? (Table 5) | Diatom data allow for, on average, >0.5 m of sudden relative sea-level rise (Table 6) | Tsunami concurrent with submergence§ | Shaking-induced liquefaction concurrent with soil burial# |
| I** | 250** | X** | X** | X** | X** | X** | X |
| II | NA†† | X | X | X | | X | |
| III | 1940–2130 | X | X | X | | X | |
| IV | NA†† | X | X | X | | X | |
| V | 2460–2750 | X | X | X | X | X | X |
| VI | 2880–3160 | X | X | X | X | X | |
| VII | 3390–3560 | X | X | X | X | X | |
| VIIa | NA†† | X | X | | | | |
| VIII | 3630–3870 | X | X | X | X | X | |
| IX | 4150–4410 | X | X | X | X | X | |
| X | 4830–5220 | X | X | X | X | X | |
| XI | 5050–5600§§ | X | X | X | X | X | |
| XII | 5750–6180§§ | X | X | X? | | X? | |

*See Table 5. All ages based on multiple radiocarbon dates unless noted in table footnotes.

†Evidence for coseismic subsidence includes abruptness of buried soil contact (Nelson et al., 1996a); lasting nature of transition from soil to mud (Hemphill-Haley, 1995; Nelson et al., 1996a); laterally extensive buried soil/mud contacts (Nelson et al., 1996a); a significant magnitude of sudden relative sea-level rise, as determined by changes in diatom assemblage across buried soil contact (Nelson et al., 1996a); tsunami concurrent with submergence (Nelson et al., 1996a); and shaking-induced liquefaction concurrent with soil burial (Atwater, 1992).

§Evidence for tsunami is sandy units abruptly deposited above soil units that were buried as a consequence of tectonic subsidence (see text).

#Evidence for liquefaction induced by strong shaking is presented for the Sixes River levee-cutbank site (see text).

**Event I is the A.D. 1700 Cascadia plate-boundary earthquake. Kelsey et al. (1998) discussed evidence of this event in the Sixes River valley.

††No $^{14}C$ age available for buried soils II, IV, and VIIa.

§§Based on one radiocarbon date.

volved intrusion of sand into the middle sedimentary sequence (Figs. 9 and 10). The second sand intrusion postdates weathering of the middle sedimentary sequence because the intrusive sand dikes follow vertical columnar ped faces in the buried soil at the top of the middle sequence. The second set of sand dikes intrudes through the older liquefied sand unit (Fig. 10). The second sand does not intrude into the youngest, upper sedimentary sequence (Fig. 9).

## DISCUSSION

### Evidence for Plate-Boundary Earthquakes

A 6000-yr-long stratigraphic record in the lower Sixes River valley reveals a suite of at least 11 buried marsh soils. Most all of the buried soils developed in high tidal marshes or freshwater marshes and were buried by tidal mud when instances of abrupt sea-level rise caused a change to a tidal-marsh or tidal-flat environment. The 11 wetland soils were abruptly submerged, on the basis of the abrupt nature of their contacts with overlying tidal mud (Tables 1 and 2). Individual buried soil horizons could be correlated over laterally extensive areas, ranging from 150 000 $m^3$ to 220 000 $m^3$ (Fig. 4; Table 5), from which we infer that successive individual relative sea-level rise events affected the entire lowland. Each relative sea-level rise was long lasting (≥70 yr) because the mud interval separating buried soils is >10 cm thick (Fig. 3; Table 3). On the basis of marsh-accretion rates (Fig. 11), 10 cm represents 70–140 yr. In addition, diatom paleoecologic data indicate that the lower-elevation diatom ecologic assemblage that formed following submergence was also long lasting (hundreds of years in the case of soils X, IX, VIII, VII, and VI, Fig. 7).

Abrupt relative sea-level rise was caused by abrupt tectonic subsidence rather than abrupt rise in ocean level. The combined abruptness and permanence of the rise, and the extensive area affected by the rise, are not characteristic effects of processes that change ocean level, which include tides, storm surge, eustatic (gradual, long term) sea-level changes, or local changes in tidal regime brought on by changes in location and geometry of beach barrier bars (Nelson et al., 1996a).

On the basis of those soils with diatom biostratigraphic data, each episode of subsidence was ~0.5 m or greater (Table 6; Fig. 7). The magnitude of subsidence for buried soils VI, VII, IX, and X could have been as much as 2.4 m. For buried soil VIII, abrupt subsidence could have been as large as 1.4 m (Fig. 7). In all instances of subsidence, relative sea-level rise was, at the least, significant enough to cause deposition of tidal mud on surfaces that formerly could support marsh vegetation.

All buried soil horizons are overlain by a sand unit, which we infer was deposited by a tsunami. Because each sand unit occurs abruptly above the buried soil and grades upward gradually to tidal mud, we infer that the deposition of sand immediately followed the abrupt subsidence. Tsunamis transported sand from the beach and nearshore marine environment onto the vegetated marsh surface. Tsunami sands on top of older, deeper buried soils are thicker and more extensive (Tables 1 and 2), indicating that tsunamis more easily invaded the lower Sixes Valley prior to ~2500 yr ago. This finding is consistent with the inference from diatom data of more brackish conditions prior to 2500 yr ago (Fig. 6). The variation in sand texture (Fig. 5) reflects differences in source area of the sediment entrained in tsunami pulses and differences in transport velocity at the site of deposition. Multiple fining-upward pulses of sand (Fig. 5) indicate successive deposition of sand from several distinct tsunami waves. Deposition of sand from storm surge or other processes that result in extreme ocean levels are not reasonable alternative modes of deposition because only tsunami satisfy the condition that each sand was deposited immediately following abrupt tectonic subsidence.

We infer that all buried soils, except buried soils VIIa and XII, are stratigraphic indicators of plate-boundary earthquakes because these soils have multiple lines of evidence implicating tectonic subsidence as the cause of soil burial (Table 7). Buried soil VIIa is an exception because it was only observed in one core (Core J in the upper meander, Fig. 3), and it has no biostratigraphic evidence for subsidence (Table 6). Buried soil VIIa could have

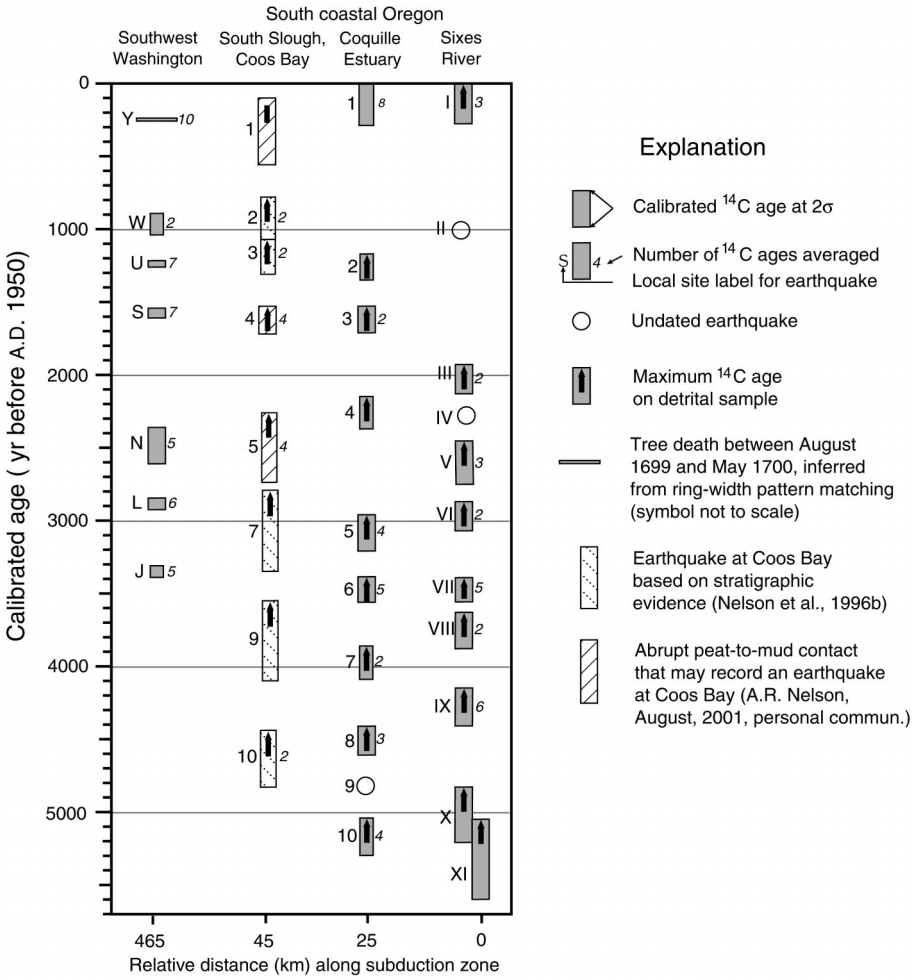


**Figure 12. Comparison of calibrated age ranges for Cascadia subduction-zone–related earthquakes at four paleoseismic sites: Sixes River (earthquake I from Kelsey et al., 1998), Coquille estuary (Witter, 1999), Coos Bay (Nelson et al., 1996b; A.R. Nelson, 2001, personal commun.), and southwest Washington (Atwater and Hemphill-Haley, 1997; B.F. Atwater, 2001, personal commun.). It is unlikely that all Cascadia subduction-zone–related earthquakes rupture the entire plate boundary from southwest Washington to southern Oregon; see text. Tree-death date for youngest earthquake from Yamaguchi et al. (1997) and Jacoby et al. (1997). All calibrated $^{14}$C ages have an error multiplier of 1.0 except Washington data where the error multiplier is 1.6.**

been caused by any one of several candidate nontectonic processes, as outlined in Nelson et al. (1996a), the most probable being a modification of the river-mouth barrier bar that affected tidal levels. Buried soil XII, which is documented in the fewest cores (Fig. 4), may record a plate-boundary earthquake; but observations are too few to convincingly argue it was formed by tectonic subsidence.

### Shaking-Induced Liquefaction

Liquefaction features in the Sixes River cutbank meet criteria proposed by Obermeier et al. (1990) for assigning a seismic origin to the liquefaction. The fluidized sand bodies show evidence of upward-directed intrusion into host sediment, and the sand bodies are not in an area where artesian discharge could create similar features. The sand bodies resemble liquefaction features documented from historical earthquakes (Sims and Garvin, 1995; Clague et al., 1997). Especially striking similarities include the geometry of a vertical sand dike attached to a sand lens deposited at the surface and the presence of the later sand intrusion cutting across the earlier extrusion of sand onto the land surface (Figs. 9 and 10).

The liquefaction features formed in discrete episodes separated by a lengthy period of time in which liquefaction features did not form. The first instance of liquefaction occurred ~2500 yr ago during subsidence of soil V. During or immediately after soil subsidence, shaking-induced liquefaction and venting of sand at the cutbank site produced the sand volcano that overlies buried soil V (Fig. 9). We infer that the second instance of liquefaction was triggered by the 1700 Cascadia earthquake. Sand liquefied by the shaking intruded into and crosscut the sand volcano (Fig. 10) and intruded the upper buried soil (soil I) at the cutbank site (Fig. 9).

### Recurrence Interval of Earthquakes

Accuracy of a mean recurrence interval for plate-boundary earthquakes at the Sixes River depends on completeness of the record. Because of uninterrupted deposition in the lower meander throughout the late Holocene, it is unlikely that there is a missing soil and thus an incomplete record. Soil II is preserved within <0.5 m of the surface in several cores (V, DD, EE, Fig. 4), leaving little room for an overlying, missing buried soil. When comparing the past 2000 yr of buried soil record at the Sixes River with a closely adjacent paleoseismic site, the Coquille estuary (Fig. 1) that is 30 km to the north (Witter, 1999), both sites have the same number of buried soils (three) in the time interval 2000 yr ago to present (Fig. 12). The Sixes record for the past 3500 yr, when compared to three other Cascadia paleoseismic records for the same time period (Fig. 12), has the same number of earthquakes or more earthquakes than the other sites. These comparative observations support the inference of no missing earthquakes.

Assuming a complete record of 11 earthquakes (I through XI), we calculate a mean recurrence interval by using the age of the youngest earthquake (A.D. 1700) and the age-range estimate for the oldest earthquake (5050–5600 cal. yr B.P., Table 5). The maximum interval of time separating earthquakes I and XI is 5350 yr, and the minimum interval of time separating them is 4800 yr; dividing each by 10 (the number of earthquakes that have occurred since earthquake XI [Table 7]) yields an average recurrence interval for 11 earthquakes of 480–535 yr.

### Folding of Cape Blanco Anticline During Plate-Boundary Earthquakes and Origin of Soil Couplets

The Cape Blanco anticline is an upper-plate structure above the Cascadia plate boundary

that deforms surfaces and sediments of late Quaternary age (Kelsey, 1990; Kelsey et al., 1996). Deformation during the 1964 Alaska earthquake (Plafker, 1969) demonstrates that structures in the upper plate of a subduction zone can grow coseismically during an earthquake on the megathrust. Is there a blind, upper-plate fault under the Cape Blanco anticline that coseismically ruptures during some of the plate-boundary earthquakes, thereby tightening the anticline? If so, then areas closest to the axis should, over the period of several subduction-zone–related earthquake cycles (thousands of years), show less subsidence than areas farther away. We compare the thickness of tidal mud and peat on top of buried marsh soils at the lower-meander site and the upper-meander site, which are 0.9–1.6 km and 2.3 km, respectively, south of the anticline axis (Figs. 1 and 2).

In the 2000 yr period between ~5000 and 3000 yr ago, more tidal mud and peat accreted in the upper meander than in the lower meander (2.91 m vs. 1.62 m) (Fig. 11). More than half of the difference in the amount of tidal mud that accreted at the upper meander versus at the lower meander is attributable to the earthquake that resulted in the tectonic subsidence of soil VII at ca. 3390–3560 cal. yr B.P. (Fig. 11).

A mechanism that could account for the difference in the amount of tidal mud that accreted at the upper meander versus at the lower meander is coseismic slip on a blind reverse fault in the upper plate that contracted the overlying Cape Blanco anticline coincident with a plate-boundary earthquake. Local coseismic uplift at the anticline axis would negate in part the regional tectonic subsidence caused by slip on the underlying megathrust, resulting in less net subsidence nearer to the anticline axis. This pattern is what the mud-accretion data show for the time after the 3390–3560 cal. yr B.P. earthquake (Fig. 11).

The two buried soil couplets in the lower meander may owe their origin to coseismic folding of the Cape Blanco anticline. Soil couplets VI and VII are separated by an average of only 14 cm, but in the upper meander, these same soils are not unusually close together (Table 3, Fig. 11). We infer that the lower-meander VII/VI soil couplet formed as a result of minimal coseismic subsidence at the time of burial of the older soil of the couplet. By implication, the upper buried soil couplet in the lower meander (soils III and IV) also may have been a product of coseismic folding of the anticline during a subduction-zone–related earthquake. Since ~3000 yr ago (time of burial of soil VI), an average of 240 cm of sediment has accumulated in the upper meander, whereas only ~180 cm of sediment has accumulated in the lower meander (Fig. 11, Table 3). We infer that the greater thickness of sediment in the upper meander was caused by ~0.6 m more subsidence in the upper meander than in the lower meander during a plate-boundary earthquake at the time of burial of soil IV. The minimal subsidence in the lower meander during the earthquake, induced by folding of the Cape Blanco anticline, caused the development of soil couplet IV/III.

### Lower Sixes Valley Plate-Boundary Earthquake Record: Comparison with Other Cascadia Sites

We compare the Sixes River valley record of plate-boundary earthquakes to the record of plate-boundary earthquakes at three other sites, southwest Washington (Atwater and Hemphill-Haley, 1997; B.F. Atwater, 2001, personal commun.), Coos Bay, Oregon (Nelson et al., 1996b; A.R. Nelson, 2001, personal commun.), and Coquille River, Oregon (Witter, 1999). Although records are of different lengths, all four sites have in common a 3500-yr-long stratigraphic record of earthquakes (Fig. 12).

The Sixes River valley stratigraphic record is not entirely correlative with the other three records. In the past 3500 yr, stratigraphic evidence of up to seven plate-boundary earthquakes is found at each site (seven at southwest Washington, six at Coos Bay, six at Coquille estuary, and seven at Sixes River; Fig. 12). Even when accounting for the undated nature of earthquakes II and IV at the Sixes sites, it is still evident that Sixes earthquake III lacks a likely correlative in southwest Washington, Coos Bay, or Coquille River (Fig. 12). Furthermore, the third-to-youngest Sixes earthquake (III) is ~600 yr too old to be correlative to the third-to-youngest earthquake in southwest Washington (earthquake U, Atwater and Hemphill-Haley, 1997). How likely is it that earthquake III is 600 yr younger than the age assigned by the two $^{14}C$ dates? Of the $^{14}C$ dates in the abandoned meander on 25 samples of material similar to that used to date earthquake III (identifiable, delicate woody debris or seeds; Table 4), all ages were stratigraphically in order in the respective cores, and all ages could be grouped with similar ages from correlative buried soils, with one exception. For the exception, the sample was 300–450 yr too old when compared to stratigraphically bracketing $^{14}C$ ages. Therefore, it is possible but unlikely that the two $^{14}C$ ages that date earthquake III both are 600 yr too old. Consequently, we infer that the third-to-oldest earthquake at the Sixes River valley sites is not the same as the third-to-oldest earthquake at southwest Washington and that the third-to-oldest earthquake at the Sixes River valley sites does not a have a likely time correlative to the north along the Cascadia subduction zone. If so, then unlike the A.D. 1700 Cascadia earthquake, some Cascadia plate-boundary earthquakes do not rupture the entire subduction zone from southern Washington to southern Oregon.

## CONCLUSION

In the past 5500 yr, 11 plate-boundary earthquakes have affected the southern Oregon coast. Ten of these earthquakes are represented by a laterally extensive buried soil within the wetland part of the lower Sixes River valley. Each earthquake buried a marsh soil and changed a high marsh or freshwater marsh to a low marsh or tide flat. The 0.5 m to as much as 2.4 m of abrupt coseismic subsidence during each earthquake is consistent with reported changes elsewhere during historic plate-boundary earthquakes (Plafker, 1969, 1972). Each of the 11 earthquakes was accompanied by a tsunami that spread sand from the beach and/or nearshore onto marsh surfaces as much as 3000 m inland from the coast. Liquefaction features formed during at least two of the earthquakes.

The Sixes wetland site lies on the south limb of an actively deforming anticline. Differential subsidence of wetland sites at different distances from the anticline axis during two plate-boundary earthquakes indicates that the anticline tightens during some earthquakes. The anticline probably is a surface fold above a blind thrust that roots in the subduction megathrust. This thrust fault may move intermittently during earthquakes on the megathrust. The two sets of buried soil couplets in the lower meander are explained by plate-boundary earthquakes that trigger localized upper-plate folding; localized folding induces differential subsidence that produces closely spaced buried soils near the fold axis.

The average recurrence interval for plate-boundary earthquakes at the lower Sixes River valley is ~480–535 yr. Comparison of the Sixes River valley earthquake record with earthquake records in south coastal Oregon and southwest Washington indicate that, unlike the A.D. 1700 Cascadia earthquake that affected the entire coast from southern British Columbia to California, some plate-boundary earthquakes do not extend into both southern Oregon and southern Washington.

## ACKNOWLEDGMENTS

Supported by National Science Foundation grant EAR-9405263 and U.S. Geological Survey NEHRP 1434-93-G-2321. Land access courtesy of Oregon State Parks. J. Bockheim, T. Dawson, M. Polenz, A.R. Nelson, R.L. Witter, and J.B. Witter provided field assistance. J. Patton provided support for graphics. A.R. Nelson assisted with compilation of $^{14}C$ data from other paleoseismic sites. Reviewed by B.F. Atwater, J.M. Bartley, S.M. Cashman, J.J. Clague, J. Lee, and A.R. Nelson.

## REFERENCES CITED

Atwater, B.F., 1987, Evidence for great Holocene earthquakes along the outer coast of Washington State: Science, v. 236, p. 942–944.

Atwater, B.F., 1992, Geologic evidence for earthquakes during the past 2000 yr along the Copalis River, south coastal Washington: Journal of Geophysical Research, v. 97, p. 1901–1919.

Atwater, B.F., and Hemphill-Haley, E., 1997, Recurrence intervals for great earthquakes of the past 3500 yr at northeastern Willapa Bay, Washington: U.S. Geological Survey Professional Paper 1576, 108 p.

Atwater, B.F., and Yamaguchi, D.K., 1991, Sudden, probable coseismic submergence of Holocene trees and grass in coastal Washington state: Geology, v. 19, p. 706–709.

Atwater, B., Nelson, A., Clague, J., Carver, G., Yamaguchi, D., Bobrowsky, P., Bourgeois, J., Darienzo, M., Grant, W., Hemphill-Haley, E., Kelsey, H., Jacoby, G., Nishenko, S., Palmer, S., Peterson, C., and Reinhart, M., 1995, Summary of coastal geologic evidence of great earthquakes at the Cascadia subduction zone: Earthquake Spectra, v. 11, p. 1–17.

Bourgeois, J., and Reinhart, M.A., 1989, Onshore erosion and deposition by the 1960 tsunami at Rio Lingue estuary, south-central Chile [abs.]: Eos (Transactions, American Geophysical Union), v. 70, p. 1331.

Clague, J.J., 1997, Evidence for large earthquakes at the Cascadia subduction zone: Reviews of Geophysics, v. 35, p. 439–460.

Clague, J.J., and Bobrowsky, P.T., 1994, Evidence for a large earthquake and tsunami 100–400 yr ago on western Vancouver Island, British Columbia: Quaternary Research, v. 41, p. 176–184.

Clague, J.J., Naesgaard, E., and Nelson, A.R., 1997, Age and significance of earthquake-induced liquefaction near Vancouver, British Columbia, Canada: Canadian Geotechnical Journal, v. 34, p. 53–62.

Darienzo, M.E., and Peterson, C.D., 1990, Episodic tectonic subsidence of late Holocene salt marshes, northern Oregon central Cascadia margin: Tectonics, v. 9, p. 1–22.

Darienzo, M.E., Peterson, C.D., and Clough, C., 1994, Stratigraphic evidence for great subduction-zone earthquakes at four estuaries in northern Oregon, U.S.A.: Journal of Coastal Research, v. 10, p. 850–879.

Dawson, A.G., 1994, Geomorphological effects of tsunami runup and backwash: Geomorphology, v. 10, p. 83–94.

Goldfinger, C., Kulm, L.D., Yeats, R.S., Applegate, B., MacKay, M.E., and Moore, G.F., 1992, Transverse structural trends along the Oregon convergent margin: Implications for Cascadia earthquake potential and crustal rotations: Geology, v. 20, p. 141–144.

Guilbault, J., Clague, J.J., and LaPointe, M., 1995, Amount of subsidence during a late Holocene earthquake—Evidence from fossil tidal marsh foraminifera at Vancouver Island, west coast of Canada: Palaeogeography, Palaeoclimatology, Palaeoecology, v. 118, p. 49–71.

Hemphill-Haley, E., 1995, Diatom evidence for earthquake-induced subsidence and tsunami 300 yr ago in southern coastal Washington: Geological Society of America Bulletin, v. 107, p. 367–378.

Jacoby, G.C., Bunker, D.E., and Benson, B.E., 1997, Tree-ring evidence for an A.D. 1700 Cascadia earthquake in Washington and northern Oregon: Geology, v. 25, p. 999–1002.

Kelsey, H.M., 1990, Late Quaternary deformation of marine terraces on the Cascadia subduction zone near Cape Blanco: Tectonics, v. 9, p. 983–1014.

Kelsey, H.M., Ticknor, R.L., Bockheim, J.G., and Mitchell, C.E., 1996, Quaternary upper plate deformation in coastal Oregon: Geological Society of America Bulletin, v. 108, p. 843–860.

Kelsey, H.M., Witter, R.C., and Hemphill-Haley, E., 1998, Response of a small Oregon estuary to coseismic subsidence and postseismic uplift in the past 300 yr: Geology, v. 26, p. 231–234.

McInelly, G.W., and Kelsey, H.M., 1990, Late Quaternary tectonic deformation in the Cape Arago–Bandon region of coastal Oregon as deduced from wave-cut platforms: Journal of Geophysical Research, v. 95, p. 6699–6713.

McNeill, L.C., Goldfinger, C., Yeats, R.S., and Kulm, L.D., 1998, The effects of upper plate deformation on records of prehistoric Cascadia subduction zone earthquakes, *in* Stewart, I.S., and Vita-Finzi, C., eds., Coastal tectonics: Geological Society [London] Special Publication 146, p. 321–342.

Minoura, K., and Nakaya, S., 1991, Traces of tsunami preserved in intertidal lacustrine and marsh deposits: Some examples from northeast Japan: Journal of Geology, v. 99, p. 265–287.

Mitchell, C.E., Vincent, P., Weldon, R.J., II, and Richards, M.A., 1994, Present-day vertical deformation of the Cascadia margin, Pacific Northwest, United States: Journal of Geophysical Research, v. 99, p. 12257–12277.

National Ocean Survey, 1977, http://www.coops.nos.noaa.gov/benchmarks/9431647.html: accessed September 2000.

Nelson, A.R., and Kashima, K.K., 1993, Diatom zonation in southern Oregon tidal marshes relative to vascular plants, foraminifera, and sea level: Journal of Coastal Research, v. 9, p. 673–697.

Nelson, A.R., Shennan, I., and Long, A.J., 1996a, Identifying coseismic subsidence in tidal-wetland stratigraphic sequences at the Cascadia subduction zone of western North America: Journal of Geophysical Research, v. 101, p. 6115–6135.

Nelson, A.R., Jennings, A.E., and Kashima, K., 1996b, An earthquake history derived from stratigraphic and microfossil evidence of relative sea level change at Coos Bay, southern coastal Oregon: Geological Society of America Bulletin, v. 108, p. 141–154.

Nelson, A.R., Ota, Y., Umitsu, M., Kashima, K., and Matsushima, Y., 1998, Seismic or hydrodynamic control of rapid late-Holocene sea-level rises in southern coastal Oregon, USA?: The Holocene, v. 8, p. 287–299.

Obermeier, S.F., and Dickenson, S.E., 2000, Liquefaction evidence for the strength of ground motions resulting from late Holocene Cascadia subduction earthquakes, with emphasis on the event of 1700 A.D.: Bulletin of the Seismological Society of America, v. 90, p. 876–896.

Obermeier, S.F., Gohn, G.S., Weems, R.E., Gelinas, R.L., and Rubin, M., 1985, Geologic evidence for recurrent moderate to large earthquakes near Charleston, South Carolina: Science, v. 227, p. 408–411.

Obermeier, S.F., Jacobson, R.B., Smoot, J.P., Weems, R.E., Gohn, G.S., Monroe, J.E., and Powars, D.S., 1990, Earthquake-induced liquefaction features in the coastal setting of South Carolina and in the fluvial setting of the New Madrid seismic zone: U.S. Geological Survey Professional Paper 1504, 44 p.

Plafker, G., 1969, Tectonics of the March 27, 1964 Alaskan earthquake: U.S. Geological Survey Professional Paper 543-I, 74 p.

Plafker, G., 1972, Alaskan earthquake of 1964 and Chilean earthquake of 1960: Implications for arc tectonics: Journal of Geophysical Research, v. 77, p. 901–925.

Satake, K., Shimazaki, K., Tsuji, Y., and Ueda, K., 1996, Time and size of a giant earthquake in Cascadia inferred from Japanese tsunami records of January 1700: Nature, v. 379, p. 246–249.

Sims, J.D., and Garvin, C.D., 1995, Recurrent liquefaction induced by the 1989 Loma Prieta earthquake and the 1990 and 1991 aftershocks: Implications for paleoseismic studies: Bulletin of the Seismological Society of America, v. 85, p. 51–65.

Soil Survey Staff, 1998, Keys to soil taxonomy (eighth edition): Washington, D.C., U.S. Department of Agriculture, Natural Resources Conservation Service, 325 p.

Stuiver, M., Reimer, P.J., Bard, E., Beck, J.W., Burr, G.S., Hughen, K.A., Kromer, B., McCormac, G., Plicht, J.v.D., and Spurk, M., 1998, INTCAL98 radiocarbon age calibration, 24,000–0 cal BP: Radiocarbon, v. 40, p. 1041–1084.

Ward, G.K., and Wilson, S.R., 1978, Procedures for comparing and combining radiocarbon age determinations: A critique: Archaeometry, v. 20, p. 19–34.

Witter, R.C., 1999, Late Holocene paleoseismicity, tsunamis and relative sea-level changes along the south-central Cascadia subduction zone, southern Oregon, U.S.A. [Ph.D. thesis]: Eugene, University of Oregon, 178 p.

Yamaguchi, D.K., Atwater, B.F., Bunker, D.E., Benson, B.E., and Reid, M.S., 1997, Tree-ring dating the 1700 Cascadia earthquake: Nature, v. 389, p. 922–923.

MANUSCRIPT RECEIVED BY THE SOCIETY MARCH 1, 2001
REVISED MANUSCRIPT RECEIVED SEPTEMBER 12, 2001
MANUSCRIPT ACCEPTED OCTOBER 12, 2001

Printed in the USA